NATIONAL ADVISORY COMMITTEE FOR AERONAUTICS

TECHNICAL NOTE 2867

HEAT AND MOMENTUM TRANSFER BETWEEN A SPHERICAL PARTICLE AND AIR STREAMS

By Y. S. Tang, J. M. Duncan, and H. E. Schweyer

University of Florida

Washington
March 1953

NATIONAL ADVISORY COMMITTEE FOR AERONAUTICS

TECHNICAL NOTE 2867

HEAT AND MOMENTUM TRANSFER BETWEEN A SPHERICAL PARTICLE AND AIR STREAMS

By Y. S. Tang, J. M. Duncan, and H. E. Schweyer

SUMMARY

Heat-transfer coefficients for a spherical particle heated by an induction coil in a moving air stream were experimentally determined for the Reynolds number range from 50 to 1000 using spheres of 1/8- to 5/8-inch diameter and air velocities from 1 to 13 feet per second. A correlation of the heat-transfer factor or Stanton number with the Reynolds number was obtained and expressed by an empirical equation. This correlation is in agreement with the values calculated from theory for the lower range of Reynolds numbers studied.

The skin-friction factor representing the momentum transfer calculated from the boundary-layer theory shows good agreement with the experimental heat-transfer factor except in the lower range of Reynolds numbers studied. The relationship $St = C_f/2$ where St is the Stanton number and C_f is the skin-friction factor is suggested for the case of an air stream flowing around a sphere.

An empirical equation relating the heat-transfer factor to the total-drag coefficient is also suggested.

INTRODUCTION

For several years, there has been considerable theoretical and experimental interest in heat transfer and momentum transfer (fluid friction) for bodies submerged in a flowing fluid. These transfers occur frequently in engineering operations. They are becoming of increased importance in catalytic operations, flow in packed beds, calcining, gas absorption, combustion chambers, and other solid-gas and liquid-gas reactions.

Johnstone, Pigford, and Chapin have made an analytical study of the heat transfer between a small spherical particle and ambient fluid stream (reference 1). Drake, Sauer, and Schaaf recently have made the same theoretical analysis following Johnstone's assumptions but using a different

method for solving the differential equation (reference 2). Their solution, which differs from Johnstone's for Reynolds numbers based on the particle diameter Re below 1000, was taken as the theoretical basis for the present investigation. An extensive survey of experimental data in the literature has been made by Williams (reference 3) and an empirical curve correlating Nu with Re was recommended for a spherical particle in an air stream. However, discrepancies between the curve and the data are quite large in the region where the Reynolds number Re is less than 1000. Furthermore, those data used were either reported by the original observers as unreliable in this range or the observations were made on a water system. Because of the difference in Prandtl number of the two fluids the results would not be expected to fall on the same curve (see reference 4). This region where the Reynolds number Re is less than 1000 was, therefore, selected for further study.

The similarities between the heat- and momentum-transfer processes at the interface of a solid and fluid have been known since Reynolds first suggested the analogy theory (reference 5). This theory has been modified by various investigators, including Colburn (references 6 and 7), Prandtl (reference 8), Taylor (reference 9), Von Kármán (references 10 to 12), and, more recently, Martinelli (references 13 and 14) and Boelter, Martinelli, and Jonassen (reference 15). It has been reported as a satisfactory principle in dealing with fluids flowing parallel to surfaces such as flat plates, conduits, or other confining surfaces (references 6, 14, and 16). Few comparisons had been made in the case of blunt objects submerged in fluids until the recent work on flow around cylinders (references 17 to 19). The difficulty in a study involving a blunt object lies in the separation of the effect of the skin friction from the total drag force exerted on the body. Sherwood, in his paper reviewing the relationship of these transfers in turbulent flow, compared the calculated friction data with heat-transfer data for flow around single cylinders and showed good agreement at certain Reynolds numbers (reference 20). However, since such a comparison for spheres had not been made previous to this investigation as far as is known, the skin friction on the surface of a sphere is calculated, and the skin-friction factor C_f is compared with the heat-transfer factor St.

Since the total-drag coefficient is measurable and is available in the literature (references 21 to 23), a correlation between the total-drag coefficient C_D and the heat-transfer factor St would be of interest. This relationsip is developed for the range of Reynolds numbers Re studied where the turbulence at the wake of the sphere is a minor factor in the total drag.

This investigation was conducted by the Department of Chemical Engineering of the University of Florida under the sponsorship and with the financial assistance of the National Advisory Committee for Aeronautics.

SYMBOLS

The symbols used for general correlations are dimensionless and may be in any consistent system of units. The experimental data are all expressed in English units and so are the computations herewith. All the symbols used are listed as follows:

A	area
A_{sep}	surface area up to separation point
A_s, A_o	cross-sectional area and surface area, respectively
B, C	constants in equation (A4)
$B(g), B_a(g)$	functions of g acording to equations (B7) and (B8), respectively
b	constant in equation (A2)
C_D	total-drag coefficient $\left(\frac{\text{Total drag force}}{(\rho U_o^2/2)A_s}\right)$
C_f	skin-friction factor $\left(\frac{\text{Total frictional force}}{(\rho U_o^2/2)A}\right)$
$C_f/2$	momentum-transfer factor
c_p	specific heat at constant pressure
D	diameter of spherical particle
g	variable defined as $\pi^2 \alpha \theta / R^2$
h	heat-transfer coefficient
h_{fc}	heat-transfer coefficient due to free convection
I_p	plate current of oscillator
k	thermal conductivity
k_s	thermal conductivity of steel
k_f	thermal conductivity of fluid

L	length of wire
ΔL	finite section of length
l	length of volume element in y-direction
m	constant
M	constant in equation (2)
Nu	Nusselt number (hD/k)
p	pressure
p_o	static pressure in undisturbed stream
P	perimeter
Pr	Prandtl number $\left(C_p\mu/k\right)$
Q	rate of total heat transferred, which is equal to rate of heat generation in particle in equilibrium state
Q_o	total heat generated per unit time in sphere with radius R_o
Q_c	rate of heat transferred by conduction
q	rate of heat transferred per unit area
q_R	rate of heat transferred by radiation per unit area
R	radius
r,θ,ϕ	spheric coordinates
r_o	perpendicular distance from axis of revolution to surface of body of revolution
R_o	outside radius of spherical particle
Re	Reynolds number based on diameter of particle $(\rho DU_o/\mu)$
St	heat-transfer factor or Stanton number $(h/C_p\rho U_o)$
T	absolute temperature; in appendix A, temperature of wire referred to surroundings
T_{air}	temperature of air stream

T_1, T_2	temperatures at stations 1 and 2, the hot and cold junctions, respectively
T_f, t_f	film temperature and fluid temperature, respectively
T_s	temperature at surface of coated thermocouple wires
t_i, t_a	initial temperature and average temperature of particle, respectively
t_c, t_s	temperature at center and at surface of particle, respectively
t, t'	temperature inside and outside of particle, respectively
t_m	temperature of fluid outside the thermal boundary layer
Δt	temperature difference between particle and main air stream
U	velocity at outside of boundary layer
U_o	average velocity of undisturbed stream
U_{max}	maximum velocity at center of column
U_{av}	average velocity over entire cross section of flow
U_r, U_θ, U_ϕ	velocity of fluid in direction of spheric coordinates r, θ, and ϕ, respectively
u	component of local velocity at any point in x-direction
v	component of local velocity at any point in y-direction
V_p	plate voltage of oscillator
x	distance parallel to surface, orthogonal coordinate
y	distance perpendicular to surface, orthogonal coordinate
α	thermal diffusivity $(k/C_p\rho)$
δ	hydrodynamic boundary-layer thickness
δ_t	thermal boundary-layer thickness
ϵ	time

μ	absolute viscosity
ν	kinematic viscosity
ρ	density
τ	skin friction or shearing stress

HEAT-TRANSFER APPARATUS

Measurements of heat transfer were made on carbon-steel spherical particles suspended in an air stream and heated by an induction coil. The arrangement of the apparatus for this study is shown by figures 1 and 2. Three particle sizes (1/8-, 1/4-, and 5/8-in. diameters) were used. A single particle was suspended by means of very fine thermocouple wires in a vertical insulated glass column through which a stream of air was blown. A high-frequency (300-kc) induction coil which was wound around a section of the column was used to generate the heat in the particle. Two sizes of glass columns (2- and 3-in. inside diameters) were used so that the value of the Reynolds number Re could be changed either by changing the size of the particle or by changing the cross section of flow while the flow rate remained within the range of the rotameter. A change of the flow pattern of the main stream at a single value of Re could also be obtained by changing the column size.

The high-frequency alternating current was generated by an oscillator (Westinghouse R-F Generator). Values of the plate voltage and current of the oscillator were used as a measurement of the energy input to the heating unit. The use of an induction coil as a heat source for the study of heat transfer was illustrated by Kramers (reference 24). This method was found advantageous because it allowed the use of an extremely small particle and avoided the difficulties that may be encountered with direct electric heating.

The flow of air was obtained from a centrifugal blower discharging into a surge tank where a constant temperature ($\pm 5^{\circ}$ F) of the air was maintained by a thermostat and entered into the glass column through a wire screen. The average velocity of the air stream in the column was measured by a calibrated rotameter and the flow rate was regulated, for each test, by a gate valve downstream from the rotameter.

The actual velocity at the center of the glass column was measured by means of a pitot tube and a diaphragm-type micromanometer (reference 25) which proved to be more satisfactory than a tilting-type inclined differential manometer (reference 26) which was initially used.

The temperature of the particle relative to the air temperature was measured by a thermocouple which was also used to support the particle, with its hot junction located inside the particle and its cold junction, in the air stream. Number 40 gage Cupron (copper, 55 percent; nickel, 45 percent) and Cromin D (nickel, 30 percent; chromium, 5 percent; and iron, 65 percent) wires were used in order to minimize the wire effect at the wake of the particle and the heat loss through conduction. Both thermocouple wires were insulated by coating with shellac. The potential difference of the thermocouple was determined by a Rubicon Precision Potentiometer. The junctions of the thermocouple were formed by electrical welding using a 6-volt direct-current source as recommended by Carbon, Kutsch, and Hawkins (reference 27). The hot junction was attached inside the particle near the center so as to have the least possible disturbance of the spheric surface. Several methods of attaching the junction were tried. The method selected as most convenient was to drill and tap a hole to the center of the particle. The thermocouple wires were then passed through a steel screw, knotted on its end, and pushed to the center of the particle by the screw which was used to plug the hole in the particle. A sectional view of the particle with the thermocouple junction attached is shown in figure 3. To insure a good contact between the body of the particle and the junction, a small drop of mercury was placed in the hole before the plug was inserted. This method has the advantage of making possible the use of the same thermocouple for the different particles except the smallest particle size used for which direct soldering of the junction to the inside of the particle was employed because of mechanical difficulties in applying the above method.

Two copper-constantan thermocouples were used to obtain the temperature of the air stream for making temperature corrections and evaluating properties of the fluid. One was placed in the test section of the column and the other at the outlet of the rotameter.

TEST PROCEDURE

The spherical particle was first placed in position inside the glass column and air was blown through the column with the flow rate controlled to a desired value which was measured by a carefully calibrated rotameter. After the flow reached a stable condition, current was applied to the heating unit. A desired constant energy input to the heating unit was obtained by adjusting the input resistance. The temperature difference was read at different intervals of time. The temperature of the particle increased until the rate of heat loss from it was equal to the rate of heat generation in the particle. About 30 to 40 minutes were usually required before this steady state of heat flow was reached. The

rate of heat transfer from the particle to the air stream was then determined from the rate of heat generation in the particle which is related to the energy input to the heating unit by an experimentally determined calibration (see section entitled "Preliminary Measurements"). Because of the small temperature difference between the particle and surroundings it was considered permissible to assume the radiation loss from the particle to be negligible in comparison with the convective transfer. However, in order to evaluate any possible errors, calculations were made for the radiation loss during cooling of the particle while it was enclosed in an evacuated glass bulb. These calculations and also a consideration of possible conduction loss through the supporting wires are treated in detail in the section entitled "Preliminary Measurements" and appendix A.

The temperature differences obtained range from 8° F to about 110° F. Greater temperature differences are not desirable because the higher the value of Δt the greater the error introduced by the evaluation of the film temperature and the evaluation of the radiation, free convection, and conduction losses. The range of temperature difference was also limited by the method of calibration used for the heating unit.

PRELIMINARY MEASUREMENTS

Thermocouple Calibration

The thermocouples used were calibrated against National Bureau of Standards standarized thermometers. When compared with the calibration tables from NBS (reference 28), the calibration for the copper-constantan thermocouple showed a discrepancy of 1 percent which is allowable according to standard practice. The copper-constantan thermocouple was made of one copper wire with two constantan wires in parallel so as to eliminate the effect of nonhomogeneity of the constantan wire (reference 29). The thermocouple made from Cupron and Cromin D and used for particle-temperature measurements was made of only two wires since it was essential to maintain minimum wire cross section.

Calibration of Heating Unit

The calibration of the heating unit was made in the same manner as the test runs previously described except that the particle was enclosed in an evacuated glass bulb, the air in the column was stationary, and the cold junction of the thermocouple was placed in a melting ice bath in a thermobottle instead of suspended in the air stream. The glass bulb was suspended inside the glass column by the thermocouple wires. If the bulb were completely evacuated, the heat loss from the particle by

convection would be eliminated and the total loss would be due to radiation if conduction along the wires is negligible. When the induction coil was energized the particle temperature increased making it possible to obtain a plot of temperature rise against time. In addition to this heating curve, a cooling curve was obtained by observing the decrease in temperature with time when no energy was supplied to the heating coil. By combining these two curves the total rate of heat generation in the particle can be determined when the mass and the specific heat of the particle are known. The calibration of the induction coil was repeated for each size of particle used since the efficiency of the unit changes with the size of the particle. The calibration curves are shown in figure 4.

It is impracticable to obtain complete evacuation and maintain it for a period of time long enough to take a series of readings for this calibration. Therefore, in the actual calibration a pressure of 7 millimeters of mercury was maintained. The heat loss due to free convection[1] inside the glass bulb was then calculated from h_{fc} at 1 atmosphere using the ratio of h_{fc} at 0.01 atmosphere to h_{fc} at 1.0 atmosphere equal to approximately 1/2. This value was based on the recent work of Gordon in which he studied the heat transfer by free convection from a piece of fine wire to the surrounding air at low pressures (reference 22). The value of h_{fc} at 1 atmosphere was approximated in the present experimental apparatus with no air blown through the column and temperature differences not large enough to cause appreciable radiation. The heat loss by radiation was then obtained by deducting the heat loss due to free convection from the total loss which was obtained from the cooling curve. The heat loss due to radiation determined from these measurements agrees fairly well with the calculated value if a value of 0.7 is used for the emissivity of the steel particle in the usual Stefan-Boltzman equation

$$q_R = (0.7)(0.173)\left[\left(\frac{T_1}{100}\right)^4 - \left(\frac{T_2}{100}\right)^4\right] \qquad (1)$$

The above equation was then used for calculating the radiation corrections for the calibration of the heating unit. The conduction loss in the thermocouple wires was considered to be negligible (see appendix A). Even if this loss were appreciable it would appear in both the calibration runs and the test runs tending to eliminate this error.

---

[1]The free-convection effect is significant when temperature difference is relatively large as in this case.

Estimation of Specific Heat

From available data it can be seen that variation of the minor components in carbon steel has negligible effect on the specific heat. A value of 0.115 Btu per pound per ^{o}F, based on the composition specified by one ball-manufacturing company, was obtained from the "Metals Handbook" (reference 30). However, since the compositions of all three particles were not available, it was desirable to have a simple calorimetric measurement of their specific heats in order to detect any significant difference of composition. A simple water calorimeter made from a thin-wall test tube with an evacuated jacket was used. Twenty milliliters of distilled water were heated to approximately 200° F and poured into the calorimeter. The steel particle was then submerged and moved up and down slowly by a mechanical device to provide agitation. A cooling curve for the water and a heating curve for the particle were obtained simultaneously by means of thermocouples. The specific heats determined in this manner for the various particles were in agreement within the experimental error and were close to 0.115.

Pitot-Tube Measurement

The velocity of the air stream at the center of the column was measured by means of a pitot-tube probe using a micromanometer to detect the pressure difference between the total- and static-pressure tubes. The velocity at the center of the column was also calculated from the average velocity obtained from a rotameter by using values of the ratio U_{max}/U_{av} at various flow conditions based on the data of Nikuradse (references 21 and 31) for the radial velocity distribution near the entrance of a column corrected for the presence of the particle at the center of the column (see reference 24).

The calculated and experimental values, compared in figure 5, show good agreement, which justifies the use of calculated values especially at low velocities where the micromanometer fails to give accurate readings because of the extremely small pressure difference of the pitot tube. (See section entitled "Precision of Measurements.")

PRECISION OF MEASUREMENTS

The accuracy of the data obtained from the measurements is affected by two types of error, systematic and random. Systematic errors were introduced in the instrumentation and its calibration, and random errors are due to inconsistent behavior of equipment and to human fallibility. While the systematic errors can be analyzed on a rational basis, the random errors can be detected only by the scattering obtained in the

correlation of data. Although every effort was made to reduce random errors to a minimum, a large number of runs were used in order to obtain compensation for this type of error.

Temperature Measurement

Since the cold junction of the thermocouple was placed in the air stream, the temperature difference between the particle and air stream was measured directly. The experimental accuracy is determined by the smallest graduation of the potentiometer reading. This gives a maximum error of 2.5 percent in the temperature readings. If an error of 1 percent is allowed for the calibration curve of the thermocouple used (see section entitled "Preliminary Measurements"), the total error will then be 3.5 percent for the temperature difference between the particle and the air stream. The effect of the location of the hot and cold junctions on the accuracy of the measurement is negligible because the temperature of the particle can be considered uniform throughout as shown in appendix B and the temperature gradient of the main stream was small compared with the temperature difference measured.

In the measurement of the air-stream temperature at the outlet of the rotameter and at the test section the temperature readings were large enough to make the experimental error insignificant.

Calibration of Heating Unit

In the calibration of the heating unit the power input to the unit was determined from the plate voltage and current of the oscillator. The maximum error, when the power input was smallest, was 6 percent. This results in the same percentage error in the heat generated in the particle since the calibration curves relating the energy input to the heating unit and the heat generated in the particle show essentially constant slopes (fig. 4). However, the fact that the maximum error was not present in most cases can be shown by reproducibility tests.

In computing the rate of heat generation Q in the particle, the slopes of the heating and cooling curve were used. Evaluation of these slopes introduced a random error which cannot be readily analyzed. This error combined with the error due to instrument readings can be determined from the maximum deviation of the data from the best curve drawn for the calibration. It is observed from figure 4 that the largest deviation of about 6 percent occurred in heating the 1/8-inch-diameter particle in the 3-inch-diameter column while in most other cases 2- or 3-percent deviations are observed. The value of Q obtained from the calibration curve will then have a maximum error less than 6 percent.

Another random error which may enter into the value of the heat generated in the particle is that caused by inconsistency in the location of the particle during the test run and during the calibration. This inconsistency, if large, would change the efficiency of the heating unit and thus invalidate the calibration. Such errors were reduced to a minimum by keeping the magnetic field strength inside the induction coil as uniform as possible for a length of column several times the diameter of the largest particle. The effect of particle position was then tested and found to be less than 3-percent deviation for a displacement of 1/4 inch along the axis of the column and about 2-percent deviation for a horizontal displacement of 1/8 inch from the center. During the test runs the variation of position was much less than these values and, therefore, the error was well within the range ±3 percent.

The maximum error in the value of Q, as well as in the measurement of temperature difference Δt, has a direct effect on the computation of the heat-transfer coefficient h and hence on the value of St. The combined error of these two quantities, Q and Δt, results in a maximum value of $\left[(1 + 0.05)/(1 - 0.035)\right] - 1$ or 9 percent when the two errors are in opposite directions.

Velocity Measurement

The average velocity of the air stream and the maximum velocity at the center of the column were determined by different means. The maximum error in the average-velocity measurement determined from the least count of the rotameter scale is about 3 percent. The maximum velocity at the center of the column was measured by means of a pitot-tube sensing element connected to a micromanometer with a design sensitivity of 0.00027 inch of water. Because of the relationship between the velocity and the pressure difference obtained from the manometer, this instrument will not give accurate measurement at velocities less than 2 feet per second. However, for air velocities greater than 2 feet per second the error becomes negligible except for error introduced by the inconsistent behavior of the apparatus. As shown in figure 5, this error is about 3 percent. This error does not enter into the final result if U_{max} is calculated from U_{av}.

The error in the velocity measurement affects both the value of St and Re but in a different manner. This effect can be determined by examining the relationship of these two dimensionless groups (fig. 6(a)) which can be approximated by the simple exponential equation

$$St = Re^{-M} \qquad (2).$$

The effect of an error of 3 percent in the velocity measurement on the relationship given by equation (2) will be about 1 percent, since the value of M is approximately 0.6. When this error is added to the other possible errors discussed previously, a maximum total error of about 10 percent is obtained.

ANALYSIS OF DATA

Typical data obtained from this investigation are presented in table I. The heat-transfer coefficient was calculated from the general equation

$$Q = hA(\Delta t) \tag{3}$$

Values of Q, the rate of heat transfer from the particle to the air stream for steady-state heat flow, were read from the calibration curves (fig. 4) of the heating unit and corrected for radiation loss by equation (1). Values of Δt were measured directly by a thermocouple in the particle, with its cold junction in the surrounding air stream. The total surface area of the spheric particle is A. It is obvious that the heat-transfer coefficient obtained in this manner is an average coefficient over the entire surface of the particle. The heat-transfer factor (Stanton number St), was computed from the heat-transfer coefficient by means of the equation

$$St = \frac{h}{c_p \rho U_o} \tag{4}$$

The heat-transfer factor was used in correlating the data with the values of the Reynolds number Re and also in the comparison of heat transfer with the skin-friction factor for the momentum-transfer phenomenon. The use of this dimensionless factor as a means of correlating heat-transfer data was suggested by McAdams and Drexel (reference 32), although most available data were presented in terms of the Nusselt number Nu.

The properties of the air were evaluated at the film temperature which was assumed to be the arithmetic average of the particle temperature and the temperature of the air stream at the test section, or

$$T_f = T_{air} + \frac{1}{2}(\Delta t) \tag{5}$$

The values of the properties of the air were based on those given in the NBS-NACA "Tables of Thermal Properties of Gases" (references 33 and 34). A correction was applied for the moisture content in the air determined by taking a humidity reading at various times during the series of test runs.

SKIN FRICTION ON SURFACE OF A SPHERE

Since momentum transfer along a surface is the result of skin friction, an evaluation of this skin friction can be used in attempting a correlation between momentum transfer and heat transfer. The direct measurement of skin friction on the surface of a sphere with a stream flow in the Reynolds number Re range of 50 to 1000 was impracticable because of the minute apparatus required for the small-size sphere used. Furthermore, since the validity of experimental data for skin friction has been questioned (reference 17) it was decided to calculate values of the skin friction for use in the proposed correlation.

For the boundary layer the Navier-Stokes equation can be simplified (reference 21) into the form

$$u \frac{\partial u}{\partial x} + v \frac{\partial u}{\partial y} = - \frac{1}{\rho} \frac{\partial P}{\partial x} + \nu \frac{\partial^2 u}{\partial y^2} \tag{6}$$

where u and v are velocities along two perpendicular axes x and y and the plane of (x,y) is the plane of motion; ρ and ν are the density and kinetic viscosity of the fluid. Since the total change of pressure along the normal to the surface throughout the boundary layer is negligible,[2]

$$- \frac{1}{\rho} \frac{\partial P}{\partial x} = U \frac{\partial U}{\partial x} \tag{7}$$

where U is the velocity in the main stream just outside the boundary layer.

---

[2]This is also generally true for a curved surface. However, when the boundary-layer thickness is fairly great, the pressure gradient across the layer that is required to balance the centrifugal force produces an appreciable pressure drop between the outside of the layer and the surface. The fundamental assumption of the boundary-layer theory will be, to this extent, violated.

These equations combined with the continuity equation

$$\frac{\partial u}{\partial x} + \frac{\partial v}{\partial y} = 0 \tag{8}$$

provide the basis for calculation for all characteristics of the boundary layer. While equations (6) and (7) were developed for two-dimensional flow, they can also be used for flow around the surface of a solid of revolution such as a sphere (see references 21 and 35). In this case, the continuity equation should have the form

$$\frac{\partial (r_o u)}{\partial x} + \frac{\partial (r_o v)}{\partial y} = 0 \tag{9}$$

where r_o is the perpendicular distance from the axis of revolution to the surface. As v is small compared with u, equation (9) can be expressed approximately as

$$\frac{\partial u}{\partial x} + \frac{\partial v}{\partial y} + \frac{u}{r_o}\frac{\partial r_o}{\partial x} = 0 \tag{10}$$

Approximate Solutions

Millikan has applied the momentum equation, which can be obtained by integrating equation (6) with respect to y between 0 and δ, to spheres and has derived, after certain simplifications, the equation (reference 35)

$$\frac{\partial}{\partial x}\int_0^\delta \rho u^2\, dy - U\frac{\partial}{\partial x}\int_0^\delta \rho u\, dy - \frac{1}{r_o}\frac{dr_o}{dx}\left(U\int_0^\delta \rho u\, dy - \int_0^\delta \rho u^2\, dy\right) = -\delta\frac{\partial p}{\partial x} - \mu\left(\frac{\partial u}{\partial y}\right)_{y=0} \tag{11}$$

where x is measured from the forward stagnation point along a meridian curve as shown in figure 7.

This equation for a sphere differs from the momentum equation for two-dimensional flow only by the terms containing $\frac{1}{r_o}\frac{dr_o}{dx}$. Hence the same equations used in the Pohlhausen-Kármán method (references 36 and 37) can be applied to the sphere if these terms are added. In the present calculation of skin friction a further modification by Holstein and Bohlen (reference 38) was used.

Velocity Distribution

In the calculation of the skin friction the velocity distribution outside the boundary layer is required as shown by the term $\frac{1}{\rho}\frac{\partial p}{\partial x}$ which is equal to $U\frac{\partial U}{\partial x}$. This velocity distribution must be experimentally determined before the calculation can be performed. Such data for spheres with values of Re in the range of 50 to 1000 are not available. However, as mentioned by Tomotika (reference 39), as long as the velocity of the undisturbed stream is below the critical value for the sphere used, the velocity distribution derived from one particular pressure-distribution curve experimentally determined for one stream velocity may be taken as representative of the velocity distribution around the sphere. As a verification of this statement, the data available in the literature for the pressure distribution surrounding a sphere and a circular cylinder (references 19, 21, and 40) are shown in figure 8. The pressure-distribution curves for cylinders are available for values of Re as low as 2800. By observation of these curves two general trends may be noted. First, although the pressure-distribution curves for various Reynolds numbers show deviations at the surface near the maximum velocity point (a minimum pressure shown in the figure), at the downstream surface all the curves tend to approach a constant pressure which is not greatly affected by the value of Re. Second, the smaller the value of Re, the sooner the pressure curve recovers from the minimum values resulting in a longer flat portion of the curve. The curves for low values of Re have only one minimum point if the minor irregularities, such as seen in curve (II), are neglected. Considering these trends, the shape of the curve for even smaller values of Re would be expected to be similar to the shape of curve (I). Furthermore, calculations of skin friction based on curves (I) and (II) show a deviation of only 3 percent for the total skin friction on the surface of a sphere. It is, therefore, considered justifiable to use curve (I) as the pressure-distribution curve for calculation of skin friction in the Re range of 50 to 1000.

Result of Calculation

The skin friction on the surface of a sphere can then be calculated for each value of x from the stagnation point to the point of separation where the boundary layer leaves the surface. The point of separation, $\theta = 86^{\circ}$, was determined from the calculation and is also indicated by the pressure-distribution curve. Beyond this point, the local skin friction is small as shown by Geidt (reference 19) and in reference 21. Because of the existence of vortex rings which become unstable (references 11 and 12) at values of Re above 150 and the fact that well-defined turbulence does not exist until much higher values of Re are attained, it is probable that the usual concept of stagnant gas films for turbulent flow is not strictly applicable to this range of Re. As an estimation, 5 percent was added to the skin friction calculated for the laminar boundary layer. This value is the same as that determined for circular cylinders by Thom (reference 21).

For the correlation of skin friction with the heat-transfer data, a dimensionless factor will be used. This factor, designated as C_f, is defined as

$$C_f/2 = \frac{\text{Total frictional force on surface}}{\rho U_o^2 A} = \frac{\int \tau \, dA}{U_o^2 A \rho} \qquad (12)$$

where A is the area, τ is the shearing stress on the surface, or $\mu\left(\frac{\partial u}{\partial y}\right)_{y=0}$, and U_o is the velocity of the undisturbed stream. The area in this equation is the total surface area of the sphere and is, therefore, different from the projected area on which the drag coefficient is generally based. Furthermore, the total frictional force has to be distinguished from the friction drag. The former is the summation of the local frictional forces (shearing force) over the whole surface, while the latter is the resultant of the frictional forces in the direction of flow of the main stream. In order to compare with the heat-transfer process on the same surface, the skin-friction factor C_f is, therefore, based on the total frictional force. The direct correlation between the heat-transfer factor and the friction drag, as suggested by previous investigators (references 20 and 41), is questionable.

The results of the point-by-point calculation of the values of $\left(\frac{\tau}{\rho U_o^2}\right)\sqrt{\text{Re}}$ were integrated graphically over the area covered by the

calculation, and then divided by the total surface area of the sphere, giving the value

$$\frac{\int_0^{A_{sep}} \left(\frac{\tau}{\rho U_o^2}\sqrt{Re}\right) dA}{A} = \frac{2\pi \int_{0^o}^{\theta=86^o} \left(\frac{\tau}{\rho U_o^2}\sqrt{Re}\right) r^2 \sin\theta \, d\theta}{4\pi r^2} = 0.63$$

Adding 5 percent for the portion of the surface beyond the separation point, this becomes

$$\frac{\int_0^{A} \left(\frac{\tau}{\rho U_o^2}\sqrt{Re}\right) dA}{A} = \left(\frac{C_f}{2}\right)(Re)^{0.5} = 0.66$$

which, after rearranging, results in the final expression

$$C_f/2 = 0.66\ (Re)^{0.5} \tag{13}$$

DISCUSSION

Comparison of Experimental Results with Previous Heat-Transfer Data

The results obtained from the present investigation are presented in figure 6(a) as a plot of St against Re and in figure 6(b) as a plot of Nu against Re. The curve in figure 6(a) is represented by the empirical equation

$$St = (3.10/Re) + \left[0.55/(Re)^{0.5}\right] \tag{14}$$

with a maximum deviation from the curve of 5 percent which is within the experimental error. For comparison the results from previous investigations on spheres are also shown in figures 6(a) and 6(b).

Williams has suggested a curve for spheres based on several sets of data reported in the literature (reference 3).[3] As previously mentioned, the application of this curve in the range of Re from 50 to 1000 is limited.

---

[3]The curve given in reference 3 was corrected according to a private communication (1950) with the author.

Kramers has made a study similar to the present one, using air as one of the mediums flowing around a sphere (reference 24). His investigation covered a Re range from 200 to 2000 and gave a curve having a slope parallel to the present results as seen in figures 6(a) and 6(b). He found a linear relationship between Nu and $(Re)^{0.5}$ which may be represented by the equation

$$Nu = 3.2 + 0.59(Re)^{0.5} \tag{15}$$

However, this equation gives consistently higher values than the present results with a deviation of 50 to 55 percent.

For comparison, equation (14), which represents the present data, can be converted to a form similar to equation (15) by using a constant value of 0.67 for Pr corrected for moisture in the ambient air. This gives the equation

$$Nu = 2.1 + 0.37(Re)^{0.5} \tag{16}$$

It is evident that at low values of Re equation (16) gives a smaller value for Nu than does equation (15), and the value is closer to 2 which has been shown (references 1 and 23) to be the limiting value of Nu as Re becomes very small. Since deviations from the theoretical value are generally considered to be due to free convection this also indicates that the effect of free convection was within the experimental error.

Ranz and Marshall (reference 42) have recently suggested the equation

$$Nu = 2.0 + 0.60(Re)^{0.5}(Pr)^{0.33} \tag{17}$$

to correlate the heat-transfer data for the system of a water drop in air. For dry air where Pr = 0.71, equation (17) becomes

$$Nu = 2.0 + 0.53(Re)^{0.5} \tag{18}$$

This can also be converted to a form comparable with equation (14) to give

$$St = (2.82/Re) + \left[0.754/(Re)^{0.5}\right] \tag{19}$$

These equations give St and Nu curves, as plotted in figures 6(a) and 6(b), parallel to the curve obtained from the present investigation, but show a maximum deviation of about 28 percent in the range of Re studied. No satisfactory explanation is offered for this deviation. However, as pointed out by Ranz and Marshall (reference 42), the reliability of this correlation depends to a great extent on the values used for the transport properties of the fluid. The values of thermal conductivity of dry air used in the present calculations were obtained from the NBS-NACA "Tables of Thermal Properties of Gases" (references 33 and 34). These values are about 3 percent higher than those used by Ranz and Marshall (reference 42).

The theoretical curve shown in figures 6(a), 6(b), and 9 was obtained by Drake, Sauer, and Schaaf (reference 2) by solving the steady-state energy-flow equation for spheres. Expressed in spherical coordinates, as illustrated in figure 7, this equation is

$$U_R \frac{\partial T}{\partial r} + U_\theta \frac{1}{r} \frac{\partial T}{\partial \theta} + \frac{U_\phi}{r \sin \phi} \frac{\partial T}{\partial \phi} =$$

$$\alpha \left[\frac{1}{r^2} \frac{\partial}{\partial r} \left(r^2 \frac{\partial T}{\partial r} \right) + \frac{1}{r^2 \sin \theta} \frac{\partial}{\partial \theta} \left(\sin \theta \frac{\partial T}{\partial \theta} \right) - \frac{1}{r^2 \sin^2 \theta} \frac{\partial^2 T}{\partial \phi^2} \right] \qquad (20)$$

In obtaining this solution, several simplifying assumptions were made among which is the assumption that the velocity of the fluid around the sphere is everywhere parallel to the surface and equal to the undisturbed velocity in the main stream, or $U_\theta = U_o$.

It is evident that this approximate solution deviates from the true solution of the energy equation when the value of Re is large enough that this assumption is no longer valid because of the fact that the fluid stream separates from the particle surface. However, at small values of Re where the velocity term does not have an appreciable effect on the result, it would be expected that this approximation will approach the true solution and, therefore, the curve will represent the true values at low values of Re. With this in mind, it is expected that the experimental curve will approach Drake's curve as Re becomes small. This is seen to be the case. This agreement also leads to the possibility of extending the present data below Re = 50.

Another analytical solution, based on the thermal-boundary-layer theory, by Kudryashev (reference 23) is

$$Nu = 2.0 + 0.33(Re)^{0.5} \tag{21}$$

This equation gives still lower values for Nu than those obtained from either equation (16) or (18).

Comparison of Skin Friction with Heat-Transfer Data

The existence of an analogy between heat transfer and momentum transfer on the interfacial surface of a solid and a flowing fluid makes it possible to correlate these two transfer phenomena. The relationships that have been found useful in the cases of fluid flow in conduits and on flat surfaces suggest the desirability of such a correlation for the case of spherical particles. In the case of fluid flowing around a blunt object, the presence of impact pressure on the surface of the object also contributes to the momentum transfer, and therefore must be distinguished from that momentum transfer due to skin friction. The term "momentum transfer" as used here refers to that part of the total transfer which is due to skin friction alone since it is this momentum transfer which is analogous to heat transfer as shown in appendix C.

The factors which are comparable in these two transfer phenomena are $C_f/2$ and St. Since the flowing medium used in this investigation is air, the Prandtl number Pr is close to 1 and the ratio $St/(C_f/2)$ can be shown to be unity.[4]

As shown in figure 9, the heat-transfer factor St curve resulting from the data obtained in this investigation lies between the theoretical curve calculated by Drake, Sauer, and Schaaf (reference 2) and the $C_f/2$ curve calculated in the section entitled "Skin Friction on Surface of a Sphere." Over most of the Re range studied the experimental curve shows better agreement with the friction-factor curve than it does with Drake's theoretical curve. The deviation between the $C_f/2$ curve and the St curve at low values of Re is explained by the increase of the boundary-layer thickness. The assumption of negligible pressure drop across the layer, used in the calculation of the skin friction, becomes invalid as the boundary layer becomes thicker. The fact that the friction

---

[4]According to Von Kármán's equation (references 11 and 12),

$$St = \frac{C_f/2}{1 + 5\sqrt{C_f/2}\left\{Pr - 1 + \log_e\left[1 + (5/6)(Pr - 1)\right]\right\}}$$

then for values of Pr between 0.71 and 1

$$St = C_f/2$$

factor at low values of Re should be higher than the values calculated by the boundary-layer theory is indicated by the curve obtained from Stokes' equation for very low values of Re.

It is of interest to note the temperature profile around an evaporating water drop as reported in the recent work of Ranz and Marshall (reference 42) who point out that the thickness of the boundary layer varies with the position on the surface of the particle and is comparable with the diameter of the drop. This would seem to invalidate the calculation of skin friction based on the assumption of a thin boundary layer. However, this variation of boundary-layer thickness of the streamlines from the particle surface and, therefore, the calculation of skin friction from the stagnation point to the point of stagnation as used in the section entitled "Skin Friction on Surface of a Sphere" remains satisfactory.

It may be pointed out that the absence of an accurate method for determining the fluid dynamics in the range of Re studied has prevented obtaining better agreement in the comparison of the momentum-transfer with the heat-transfer factor.

The above considerations seem to indicate the existence of the relationship $St = C_f/2$ as expected from theoretical analysis (see appendix C). This is also in agreement with Sherwood's findings in the case of a cylinder (reference 20). In both cases the relationship applies for gases where Pr is close to unity. The existence of this simple relationship between heat and momentum transfer for a spherical particle in a gas stream discloses an additional application of the theory of analogy between these two transfer phenomena. It should be expected that this analogy would apply to any blunt object having a smooth surface in addition to its application to streamline bodies and flat or curved surfaces.

Although there is no apparent analogy between the drag coefficient C_D and the heat-transfer factor St in the Re range studied, they both show similar behavior in varying with Re. This is believed to be due to the fact that the form drag does not have a significant effect on the variation of total drag with change in Re since the air-stream velocity in this Re range is far below the critical value and, therefore, turbulence at the wake of the sphere is not an essential factor. The total-drag coefficient thus varies with Re in approximately the same manner as the surface friction drag. Since the total-drag coefficient is measurable and is available in the literature (references 21, 43, and 44), an empirical relationship between C_D and St, based on the present data, was developed (see fig. 10) resulting in the equation

$$St = (C_D/8) - \left[0.10/(Re)^{0.15}\right] \qquad (22)$$

The maximum deviation of this equation from the St curve obtained from the present experimental data is about 8 percent which is within the experimental error. Such an empirical correlation between the heat-transfer factor and total-drag coefficient may be useful for the determination of heat-transfer rates from drag measurements especially in the case of submerged bodies which are not true spheres. Such application may be valid where a correction factor (or form factor) is employed in the above equation to allow for nonsphericity.

CONCLUSIONS

The conclusions which can be drawn concerning heat and momentum transfer for the system of a spherical particle in a moving air stream, based on the results obtained in this investigation, are:

1. A correlation of the heat-transfer factor St against the Reynolds number based on particle diameter Re was obtained for the range of Re from 50 to 1000. This correlation is represented by the equation

$$St = (3.10/Re) + \left[0.55/(Re)^{0.5}\right]$$

At the extremes of the limits for the Re range studied the experimental data are in agreement with values predicted by theory which tends to substantiate the validity of the experimental curve.

2. Extension of the experimental curve into the region below values of Re of 50 by means of Drake's theoretical equation is indicated.

3. The satisfactory agreement between the calculated values of the momentum-transfer factor $C_f/2$, where C_f is the skin-friction factor, and the experimental data at the higher values of Re studied suggests the relationship $St = C_f/2$ for the case of air flowing around a sphere.

4. For practical application in the Re range of 50 to 1000, the empirical equation

$$St = (C_D/8) - \left[0.10/(Re)^{0.15}\right]$$

relating the heat-transfer factor to the readily measurable total-drag coefficient C_D may be useful for particles deviating slightly from true spherical shape.

University of Florida
Gainesville, Fla., December 10, 1951

APPENDIX A

HEAT LOSS THROUGH SUSPENSION WIRES

The conduction losses along the thermocouple wires were minimized by using extremely fine wires. However, for precision the magnitude of these losses is considered. The losses due to conduction to the ends of the wires include losses from the shellac-coated wire surface by convection and radiation. Thus the maximum loss by conduction would be

$$Q_c = -kA_s(dT/dL)_{L=0} \tag{A1}$$

The Fourier equation for conduction (reference 45) can be written as

$$\frac{\partial T}{\partial \epsilon} = \alpha \frac{\partial^2 T}{\partial L^2} - b^2 T \tag{A2}$$

where the term b^2T represents the rate of heat loss through the surface element to the surrounding medium, b^2 is a constant to be determined, ϵ is time, and T is the temperature of the wires referred to that of the surrounding medium. For steady-state heat flow, this reduces to

$$\frac{\partial^2 T}{\partial L^2} = \frac{b^2}{\alpha} T \tag{A3}$$

Equation (A3) can be solved by substituting e^{mL} for T. This results in the solution

$$T = Be^{bL/\sqrt{\alpha}} + Ce^{-bL/\sqrt{\alpha}} \tag{A4}$$

where B and C are constants. The boundary conditions for the longitudinal temperature distribution along the wires are $T = 0$ at $L = \infty$ and $T = \Delta t$ at $L = 0$.

Therefore, $B = 0$, $C = \Delta t$, and

$$T = (\Delta t)\left(e^{-bL/\sqrt{\alpha}}\right) \tag{A5}$$

from which

$$(dT/dL)_{L=0} = -(\Delta t)b/\sqrt{\alpha} \tag{A6}$$

In order to find the value of b, consider a finite section of length ΔL of the wires. A heat balance can be written as

$$kA_s \frac{d^2T}{dL^2} \Delta L = hT_s P \Delta L \tag{A7}$$

or

$$\frac{d^2T}{dL^2} = \frac{hP}{kA_s} T_s \tag{A8}$$

where h is the sum of radiation and convected film conductance which is assumed to be constant over the range of temperature considered, P and A_s are the perimeter and the cross-section area, respectively, and T_s is the temperature at the surface of the coated wires. By combining equations (A3) and (A8), b^2 can be expressed as

$$b^2 = \frac{\alpha hP}{kA_s}(T_s/T) \tag{A9}$$

The value of T_s/T determined from a heat balance across the shellac film is about 0.5, assuming a value of 15 for h at the surface of the shellac film (based on the data of Gordon (reference 22)). By substituting the proper values of P, A_s, h, and k, equation (A9) gives

$$b/\sqrt{\alpha} = 90 \text{ ft}^{-1}$$

Then

$$\left(\frac{dT}{dL}\right)_{L=0} = -90(\Delta t)$$

and

$$Q_c = kA_s(90)(\Delta t)$$

Under the test condition such that the minimum amount of heat (0.030 Btu/hr) is transferred corresponding to a value of Δt of 10° F, the conduction loss will have the maximum effect. This maximum error in the value of Q due to conduction loss may reach 3 percent. In most cases the amount of heat lost by conduction was found to be negligible.

APPENDIX B

TEMPERATURE INSIDE STEEL PARTICLE

Temperature Gradient during Heating

It is well-known that when a metallic particle is heated by an induction coil, the eddy current induced in the particle is concentrated on the surface and the interior of the metal receives heat from the skin by thermal conduction. Because of the high conductivity of steel the heat per unit volume generated in any concentric spherical element is assumed to be the same as for any other element. Thus,

$$Q/\pi R^3 = Q_o/\pi R_o^3 \tag{B1}$$

where Q_o is the total heat generated per unit time in the sphere with a radius of R_o and Q is the heat generated per unit time in a concentric sphere with radius of R, which is smaller than R_o. If A_o is the surface area of the sphere and A is that of any concentric sphere with a radius of R, then

$$\frac{Q}{A} = \frac{Q}{A}(A_o/A_o) = \frac{Q_o}{A_o}\left(\frac{R}{R_o}\right)^3\left(\frac{4\pi R_o^2}{4\pi R^2}\right) = \frac{Q_o}{A_o}\left(\frac{R}{R_o}\right) \tag{B2}$$

From Fourier's law for steady conduction

$$\frac{-dt}{dR} = \frac{Q}{k_s A} = \frac{Q_o}{A_o}\frac{R}{R_o}\frac{1}{k_s} \tag{B3}$$

Then

$$\int_{t_s}^{t} dt = -\frac{Q_o}{A_o}\left(\frac{1}{k_s R_o}\right)\int_{R_o}^{R} R\, dR$$

or

$$t - t_s = \frac{Q_o}{A_o}\left(\frac{R_o^2 - R^2}{2R_o}\right)\left(\frac{1}{k_s}\right) \tag{B4}$$

where t_s is the surface temperature of the spherical particle and k_s is the thermal conductivity of the particle. At equilibrium, when a steady state is established, the heat generated is equal to that transferred to the ambient air stream

$$Q_o/A_o = h(\Delta t)$$

where Δt is the temperature difference between the particle and the main air stream. Substituting this value in equation (B4) gives

$$t - t_s = (\Delta t)\frac{h}{k_s}\left(\frac{R_o^2 - R^2}{2R_o}\right) \tag{B5}$$

Let t_c be the temperature at the center of the sphere. Then

$$t_c - t_s = (\Delta t)\frac{hR_o}{2k_s} = (\Delta t)\left(\frac{hR_o}{2k_f}\right)\left(\frac{k_f}{k_s}\right) \tag{B6}$$

where k_f is the thermal conductivity of the ambient fluid. It is evident that k_f for air is much smaller than k_s (k_f/k_s is approximately 1/2000) and since the value of Nu which is equal to $2hR_o/k_f$ is never more than 20 for the range of Re studied, the value of $t_c - t_s$ is less than 0.25 percent of Δt.[5] Hence the error introduced by considering t_c equal to t_s is negligible for the values of Δt encountered in this investigation.

Temperature Gradient during Cooling

In calibrating the heating unit, cooling curves of the particle as well as heating curves were used. The fact that the temperature measured by attaching a thermocouple at the center of the particle can be used in place of the surface temperature must be established.

To determine the possible error introduced by the assumption of a uniform temperature within the particle at any instant the temperature of the rarefied gas surrounding the particle inside the evacuated bulb is assumed to be uniform and equal to the surface temperature t_s. If

[5]Since the temperature at the surface equals the temperature at the center a uniform temperature must exist throughout the particle which justifies the original assumption made for the heat distribution.

t_s is suddenly reduced to some temperature lower than the initial temperature of the particle[6] there will be an instantaneous temperature gradient established within the particle because of the thermal resistance to the conduction of heat from the center to the surface of the particle. Then, from the Fourier equation of conduction (reference 45),

$$\frac{t_c - t_s}{t_i - t_s} = 2\left(e^{-g} - e^{-4g} + e^{-9g} - \ldots\right) \equiv B(g) \qquad (B7)$$

and

$$\frac{t_a - t_s}{t_i - t_s} = \frac{6}{\pi^2}\left(e^{-g} + \frac{1}{4}e^{-4g} + \frac{1}{9}e^{-9g} + \ldots\right) \equiv B_a(g) \qquad (B8)$$

where t_c is the temperature at the center of the particle, t_i is the initial uniform temperature of the particle, t_a is the average temperature of the particle at time ϵ, and g is defined by

$$g = \pi^2 \alpha \epsilon / R_o^2$$

If the time interval ϵ is 2 seconds and the thermal diffusivity α of steel is 0.570 square foot per hour, then for the largest spherical particle used (R_o = 5/16 in.)

$$g = 4.61$$

From the table of values for the functions $B(g)$ and $B_a(g)$, (reference 45), it is found that

$$B(g) = 0.020$$

$$B_a(g) = 0.006$$

Then, by combining equations (B7) and (B8),

$$(t_a - t_s) - (t_c - t_s) = (0.020 - 0.006)(t_i - t_s)$$

Thus the error in this case which would be the maximum error encountered in the tests will be 1.4 percent of the temperature change from the initial temperature to the surface temperature.

---

[6]This is a hypothetical condition which represents the most unfavorable condition resulting in maximum error.

APPENDIX C

HEAT- AND MOMENTUM-TRANSFER ANALOGY

Considering a laminar boundary layer on the surface of a sphere where no fluctuations in velocity and temperature exist, the analogy between heat and momentum transfer (references 11 and 12) can be seen from the similarity in form of the following equations. For heat transfer

$$q/c_p\rho = -\alpha \frac{dt}{dy} \tag{C1}$$

and for momentum transfer

$$\tau/\rho = \nu \frac{du}{dy} \tag{C2}$$

where y is in a direction perpendicular to the surface.

These two equations will be directly proportional if ν and α are numerically equal, or

$$\nu/\alpha = \mu c_p/k = Pr = 1$$

which is approximately satisfied by a gas. If in this layer q and τ are assumed to vary with y in a similar manner, the velocity and temperature at the boundary are U_o and t_m, respectively, and t' is the temperature of the fluid referred to a surface temperature of zero, then

$$-\int_0^{t_m} \frac{dt'}{(q/c_p\rho)} = \int \frac{dy}{\alpha} \tag{C3}$$

$$\int_0^{U_o} \frac{du}{(\tau/\rho)} = \int \frac{dy}{\nu} \tag{C4}$$

Therefore,

$$U_o/(\tau/\rho) = c_p\rho(\Delta t)/q \tag{C5}$$

By using the definitions of the skin-friction factor $C_f = \tau/\left(\rho U_o^2/2\right)$ and heat-transfer factor $St = h/c_p\rho U_o = q/c_p\rho U_o(\Delta t)$, the above relationship can be transformed into the familiar form

$$C_f/2 = St \tag{C6}$$

This relationship was derived on the assumption that the boundary layer for the velocity field is the same as that for the thermal field. This is true, however, only for gases. In general the hydrodynamic boundary layer and the thermal boundary layer have different thicknesses, δ and δ_t, respectively. For the determination of the thermal-boundary-layer thickness and the heat transfer through this layer, a heat-flow equation for the thermal boundary layer can be used. The desired equation is derived from a heat balance for a volume element of the fluid at the surface of the sphere, similar to the derivation of the momentum equation for the hydrodynamic boundary layer:

$$\rho c_p \frac{d}{dx}\int_0^l t_f u\, dy - \rho c_p \frac{d}{dx}\int_0^l t'u\, dy - k\left(\frac{dt'}{dy}\right)_{y=0} = 0 \tag{C7}$$

where t_f is the temperature of the undisturbed stream and l, the length of the volume element in the y-direction, is assumed to be greater than either δ or δ_t. By introducing the thermal diffusivity of the fluid $\alpha = k/c_p\rho$, equation (C7) becomes

$$\frac{d}{dx}\int_0^l (t_f - t')u\, dy = \alpha\left(\frac{dt'}{dy}\right)_{y=0} \tag{C8}$$

By assuming the temperature profile in terms of y/δ_t to be analogous to the velocity profile in terms of y/δ and $(\delta_t/\delta) < 1$, the value of δ_t/δ can be obtained (reference 4):

$$\delta_t/\delta = 1/(Pr)^{1/3} \tag{C9}$$

Since Pr for gases is smaller than 1, δ_t/δ becomes greater than 1, and the assumption made in obtaining equation (C9) is not strictly true. However, the error introduced by this approximation when the Prandtl number is close to 1 is very small, giving a value for δ_t/δ of approximately 1.1. It is, therefore, considered satisfactory to assume δ_t equal to δ in the analogy equation, with a possible error of 10 percent.

REFERENCES

1. Johnstone, H. F., Pigford, R. L., and Chapin, J. H.: Heat Transfer to Clouds of Falling Particles. Bull. No. 330, Eng. Exp. Station, Univ. of Ill., vol. 38, no. 43, June 17, 1941.

2. Drake, R. M., Jr., Sauer, F. M., Jr., and Schaaf, S. A.: Forced Convection Heat Transfer from Cylinders and Spheres in a Rarefied Gas. Rep. No. HE-150-74, Contract No. N7-onr-295-Task 3, Inst. Eng. Res., Univ. of Calif., Nov. 15, 1950.

3. Williams, Glenn Carber: Heat Transfer, Mass Transfer and Friction for Spheres. D. Sc. Thesis, M.I.T., Sept. 1942.

4. Eckert, Ernst: Introduction to the Transfer of Heat and Mass. First ed., McGraw-Hill Book Co., Inc., 1950.

5. Reynolds, O.: On the Extent and Action of the Heating Surface for Steam Boilers. Proc. Manchester Literary Phil. Soc., vol. 8, Oct. 1874, p. 7; reprinted in "Scientific Papers of Osborne Reynolds." Vol. 1. Cambridge Univ. Press (London), 1900, pp. 81-85.

6. Colburn, Allan P.: A Method of Correlating Forced Convection Heat Transfer Data and a Comparison with Fluid Friction. Trans. Am. Inst. Chem. Eng., vol. 29, June 15, 1933, pp. 174-210.

7. Colburn, Allan P.: Heat Transfer by Natural and Forced Convection. Res. Ser. No. 84, Eng. Bull., Purdue Univ., vol. XXVI, no. 1, Jan. 1942.

8. Prandtl, L.: Ein Beziehung zwischen Wärmeaustausch und Strömungswiderstand der Flüssigkeiten. Zeitschr. Phys., Bd. 11, Heft 23, Nov. 1910, pp. 1072-1078; Bemerkung über den Warmeubergang im Rohr. Zeitschr. Phys., Bd. 29, Heft 14, July 1928, pp. 487-489.

9. Taylor, G. I.: Conditions at the Surface of a Hot Body Exposed to the Wind. R. & M. No. 272, British A.R.C., 1916.

10. Von Kármán, Th.: Über Laminare und turbulente Reibung. Z.a.M.M., Bd. 1, Heft 4, Aug. 1921, pp. 233-251.

11. Von Kármán, Th.: The Analogy between Fluid Friction and Heat Transfer. Trans. A.S.M.E., vol. 61, no. 8, Nov. 1939, pp. 705-710.

12. Von Kármán, Th.: Analogy between Fluid Friction and Heat Transfer. Engineering, vol. 148, no. 3840, Aug. 18, 1939, pp. 210-213.

13. Martinelli, R. C.: Heat Transfer to Molten Metals. Trans. A.S.M.E., vol. 69, no. 8, Nov. 1947, pp. 947-956; discussion, pp. 956-959.

14. Martinelli, R. C.: Further Remarks on the Analogy between Heat and Mometum Transfer. Paper presented at annual meeting of A.S.M.E., Dec. 1946.

15. Boelter, L. M. K., Martinelli, R. C., and Jonassen, Finn: Remarks on the Analogy between Heat Transfer and Momentum Transfer. Trans. A.S.M.E., vol. 63, no. 5, July 1941, pp. 447-455.

16. Rubesin, M. W., and Johnson, H. A.: A Critical Review of Skin-Friction and Heat-Transfer Solutions of the Laminar Boundary Layer of a Flat Plate. Trans. A.S.M.E., vol. 71, no. 4, May 1949, pp. 383-388.

17. Drake, R. M., Jr.: An Investigation of the Skin Friction and Heat Transfer for an Arbitrary Body in the Case of a Laminar Boundary Layer. Ph. D. Thesis, Univ. of Calif., 1950.

18. Giedt, W. H.: A Study of Local Heat Transfer and Skin Friction on a Circular Cylinder in the Critical Flow Range. Ph. D. Thesis, Univ. of Calif., 1950.

19. Giedt, W. H.: Investigation of Variation of Point Unit Heat-Transfer Coefficient around a Cylinder Normal to an Air Stream. Trans. A.S.M.E., vol. 71, no. 4, May 1949, pp. 375-381.

20. Sherwood, T. K.: Heat Transfer, Mass Transfer, and Fluid Friction. Ind. and Eng. Chem., vol. 42, no. 10, Oct. 1950, pp. 2077-2084.

21. Fluid Motion Panel of the Aeronautical Research Committee and Others (S. Goldstein, ed.): Modern Developments in Fluid Dynamics. Vols. I and II. First ed., The Clarendon Press (Oxford), 1948.

22. Gordon, H. S.: Heat Transfer by Free Convection from Small Diameter Wires. Ph. D. Thesis, Univ. of Calif., 1950.

23. Kudryashev, L. I.: A Refinement of the Calculation of the Heat Transfer Coefficient between Gas and Suspended Particles by Application of the Thermal Boundary Layer Method. Izvestiya Akad. Nauk U.S.S.R., Otdelenie Tekh. Nauk, no. 11, 1949, pp. 1620-1625. Translated by M. Goyer, Lib. Translation No. 368, British R.A.E. (Farnborough), March 1951.

24. Kramers, H.: Heat Transfer from Spheres to Flowing Media. Physica, vol. 12, no. 2-3, June 1946, pp. 61-80.

25. Dibeler, Vernon H., and Cordero, Fidel: Diaphragm-Type Micromanometer for Use on a Mass Spectrometer. Res. Paper RP 2167, Jour. Res., Nat, Bur. Standards, vol. 46, no. 1, Jan. 1951, pp. 1-4.

26. Pannell, J. R.: Fluid Velocity and Pressure. First ed., Edward Arnold Co. (London), 1924.

27. Carbon, M. W., Kutsch, H. J., and Hawkins, G. A.: The Response of Thermocouples to Rapid Gas-Temperature Changes. Trans. A.S.M.E., vol. 72, no. 5, July 1950, pp. 655-657.

28. Roeser, W. M. F., and Dahl, Andrew I.: Reference Tables for Iron-Constantan and Copper-Constantan Thermocouples. Res. Paper RP 1080, Jour. Res., Nat. Bur. Standards, vol. 20, no. 3, March 1938, pp. 337-355.

29. Scott, R. B.: The Calibration of Thermocouples at Low Temperatures. Temperature, Its Measurement and Control in Science and Industry. First ed., Reinhold Pub. Co., 1941.

30. Lyman, Taylor, ed.: Metals Handbook. Am. Soc. Metals (Cleveland), 1948.

31. Tietjens, Oskar G.: Applied Hydro- and Aeromechanics. First ed., McGraw-Hill Book Co., Inc., 1934.

32. Drexel, Roger E., and McAdams, William H.: Heat-Transfer Coefficients for Air Flowing in Round Tubes, in Rectangular Ducts, and around Finned Cylinders. NACA ARR 4F28, 1945.

33. Morey, F. C.: Dry Air. NBS-NACA Tables of Thermal Properties of Gases, Table 2.39, July 1950.

34. Hilsenrath, Joseph: Dry Air. NBS-NACA TAbles of Thermal Properties of Gases, Table 2.44, July 1950.

35. Millikan, Clark B.: The Boundary Layer and Skin Friction for a Figure of Revolution. Trans. A.S.M.E., vol. 54, no. 3, Jan. 30, 1932, pp. 29-43.

36. Pohlhausen, K.: Zur näherungsweisen Intergration der Differentialgleichungen der laminaren Reibungsschicht. Z.a.M.M., Bd. 1, Heft 4, Aug. 1921, pp. 252-268.

37. Schlichting, H.: Vortragsreihe "Grenzschichttheorie." Teil A: Laminare Strömungen. Z.W.B. (Berlin-Adlershof), 1941/42, pp. 1-153. Translated as NACA TM 1217, 1949.

38. Holstein-Bolen: Ein Vereinfachtes Verfahren zur Berechnung Laminarer Reibungsschichten, die dem Nächerungsansatz von K. Pohlhausen genügen.

39. Tomotika, S.: The Laminar Boundary Layer on the Surface of a Sphere in a Uniform Stream. R. & M. No. 1678, British A.R.C., 1936.

40. Flachsbart, O.: Neue Untersuchungen über den Luftwiderstand von Kugeln. Zeitschr. Phys., Bd. 28, Heft 13, July 1927, pp. 461-469.

41. Boelter, L. M. K., Cherry, V. H., Johnson, H. A., and Martinelli, R. C.: Heat Transfer Notes. Univ. of Calif. Press (Berkeley), 1948.

42. Ranz, W. E., and Marshall, W. R.: Evaporation from Drops. Chem. Eng. Progress, vol. 48, no. 4, April 1952, pp. 173-180.

43. Lapple, C. E., and Shepherd, C. B.: Calculation of Particle Trajectories. Ind. and Eng. Chem., vol. 32, no. 5, May 1940, pp. 605-617.

44. Zahm, A. F.: Flow and Drag Formula for Simple Quadrics. NACA Rep. 253, 1927.

45. Ingersoll, Leonard R., Zobel, Otto J., and Ingersoll, Alfred C.: Heat Conduction with Engineering and Geological Applications. First ed., McGraw-Hill Book Co., Inc., 1948.

TABLE I

EXPERIMENTAL RESULTS[1]

Run number[2]	A-201	A-210	A-215	A-224	A-229	A-231	A-239	A-246	A-303	A-306	A-312	A-318	A-323	A-327	A-333	A-342
Rotameter reading, cu ft/min	1.4	1.6	2.0	2.5	3.0	4.0	5.0	6.0	1.4	2.0	2.5	3.0	4.0	6.0	8.0	10.0
Thermocouple reading (I), mv	1.270	1.329	1.321	1.362	1.327	1.269	1.511	1.450	1.520	1.445	1.413	1.613	1.725	1.478	1.635	1.778
Air temperature at rotameter outlet, ^{o}F	90.4	93.1	92.7	94.5	93.0	90.3	100.6	99.4	101.4	98.2	96.4	105.5	110.4	99.6	106.4	112.6
Thermocouple reading (II), mv	1.225	1.206	1.185	1.390	1.122	1.119	1.283	1.338	1.376	1.290	1.286	1.415	1.352	1.362	1.411	1.298
Air temperature at test section, ^{o}F	88.6	87.6	86.8	91.3	83.8	83.6	91.0	93.5	95.1	91.3	91.1	96.8	94.0	94.5	96.5	91.6
Air velocity at particle cross section, ft/sec	2.00	2.23	2.69	3.26	3.78	4.45	5.40	6.42	0.86	1.20	1.46	1.71	2.18	3.10	3.84	4.63
Power input to heating unit, volt amperes	20.0	34.0	27.0	49.2	70.0	27.9	41.3	70.0	63.0	49.2	49.2	71.2	63.0	40.2	32.5	63.0
Rate of heat transfer, Q, Btu/hr	0.032	0.057	0.043	0.094	0.147	0.047	0.077	0.150	0.079	0.056	0.056	0.092	0.080	0.042	0.030	0.081
Thermocouple reading (III), mv	0.228	0.357	0.273	0.515	0.730	0.220	0.335	0.600	0.624	0.390	0.384	0.614	0.484	0.236	0.153	0.370
Temperature difference, Δt, ^{o}F	11.6	18.0	13.9	26.2	37.1	11.2	17.0	30.4	31.6	19.7	19.5	31.2	24.5	12.2	7.9	18.6
Film temperature, ^{o}F	94.4	96.6	93.8	104.4	102.4	89.2	102.0	107.3	110.9	101.2	100.9	112.4	106.3	100.6	100.4	100.9
Reynolds number, Re	122	137	165	195	230	277	332	377	50	71	90	99	128	181	230	277
Heat-transfer coefficient h, $Btu/ft^2/hr/^{o}F$	8.10	9.30	9.10	10.5	11.70	12.3	13.3	14.5	7.35	8.34	8.24	8.65	9.58	10.1	11.2	12.8
Heat-transfer factor, St	0.066	0.068	0.054	0.052	0.051	0.044	0.040	0.037	0.142	0.115	0.092	0.085	0.070	0.055	0.048	0.045
Nusselt number, Nu	5.4	6.1	6.0	6.8	7.7	8.2	8.7	9.4	4.8	5.5	5.4	5.6	6.2	6.6	7.4	8.4

[1]Only typical runs are listed. The complete table of data is available in the unpublished copy of the annual report to NACA from the Univ. of Florida submitted under contract NAw-6018 and entitled: "A Special Analytical Study of Heat Transfer Phenomena with Clouds of Small Particles in Air at Elevated Temperatures. Part I: Study of Heat Transfer with Single Particles" by J. M. Duncan, Y. S. Tang, C. R. Wallace, and C. M. Oktay. This report is available for loan or reference in the Division of Research Information, National Advisory Committee for Aeronautics, Washington, D. C.

[2]Designations: A - particle size, 1/8 in.; B - particle size, 1/4 in.; C - particle size, 5/8 in. Run number in 200 series represents 2-in. I.D. of glass column used and run number in 300 series represents 3-in. I.D. of glass column used.

TABLE I - Concluded

EXPERIMENTAL RESULTS

Run number[2]	B-201	B-205	B-210	B-214	B-219	B-224	B-302	B-306	B-307	B-311	B-317	B-325	B-331	C-202	C-204	C-301	C-304	C-308	C-310	C-315
Rotameter reading, cu ft/min	2.0	4.0	6.0	8.0	10.1	12.0	2.0	4.0	6.0	8.0	10.0	12.0	13.0	2.0	4.0	3.0	4.0	5.0	6.0	8.0
Thermocouple reading (I), mv	1.320	1.402	1.383	1.390	1.468	1.462	1.484	1.642	1.633	1.572	1.637	1.695	1.534	1.465	1.515	1.425	1.416	1.528	1.569	1.695
Air temperature at rotameter outlet, °F	92.6	96.2	95.9	95.8	99.1	98.8	99.9	106.8	106.5	103.7	106.5	110.1	102.1	99.0	101.2	97.2	96.8	101.8	103.6	109.1
Thermocouple reading (II), mv	1.187	1.189	1.227	1.180	1.262	1.362	1.290	1.350	1.343	1.365	1.412	1.485	1.225	1.293	1.370	1.173	1.295	1.300	1.288	1.340
Air temperature at test section, °F	86.8	87.0	88.7	86.6	90.1	94.5	91.3	94.0	93.7	94.6	96.6	100.0	88.6	91.4	94.9	86.0	91.6	91.8	91.2	93.6
Air velocity at particle cross section, ft/sec	2.70	4.53	6.54	8.32	10.30	12.22	1.21	2.17	3.00	3.87	4.76	5.64	5.99	2.82	4.72	1.73	2.22	2.84	3.07	3.92
Power input to heating unit, volt amperes	27.0	32.5	46.8	48.8	53.1	66.5	18.0	22.5	18.5	22.5	27.5	34.1	42.0	10.5	28.5	20.0	10.5	10.5	20.0	25.8
Rate of heat transfer, Q, Btu/hr	0.34	0.47	0.75	0.72	0.81	1.18	0.15	0.21	0.17	0.22	0.30	0.39	0.49	1.00	4.40	1.70	0.35	0.35	1.82	2.72
Thermocouple reading (III), mv	0.765	0.870	1.295	1.220	1.055	1.410	0.452	0.572	0.383	0.446	0.560	0.698	0.860	0.730	0.260	1.449	0.245	1.230	1.132	0.555
Temperature difference, Δt, °F	38.9	44.3	65.8	62.0	53.6	70.9	22.9	29.1	19.5	22.6	28.4	35.6	43.7	37.1	110.6	72.9	12.6	11.8	57.6	78.3
Film temperature, °F	106.3	109.2	121.6	117.5	116.9	130.0	102.8	108.6	103.6	105.9	111.0	117.8	110.5	110.0	150.2	122.5	97.9	97.7	120.0	132.8
Reynolds number, Re	320	531	736	952	1172	1340	143	254	355	455	554	644	699	825	1226	486	674	830	870	1070
Heat-transfer coefficient, h, Btu/ft²/hr/°F	6.41	7.82	8.47	8.5	11.1	12.4	4.81	5.30	6.40	7.15	7.75	8.05	8.30	3.15	4.65	2.72	3.25	3.47	3.70	4.07
Heat-transfer factor, St	0.039	0.029	0.022	0.018	0.019	0.017	0.065	0.041	0.036	0.031	0.028	0.025	0.023	0.019	0.017	0.027	0.024	0.020	0.021	0.018
Nusselt number, Nu	8.3	10.1	10.8	10.9	14.2	15.6	6.3	6.9	8.4	9.3	10.0	10.3	10.7	10.2	14.2	8.6	10.7	11.4	11.8	12.7

[2]Designations: A - particle size, 1/8 in.; B - particle size, 1/4 in.; C - particle size, 5/8 in. Run number in 200 series represents 2-in. I.D. of glass column used and run number in 300 series represents 3-in. I.D. of glass column used.

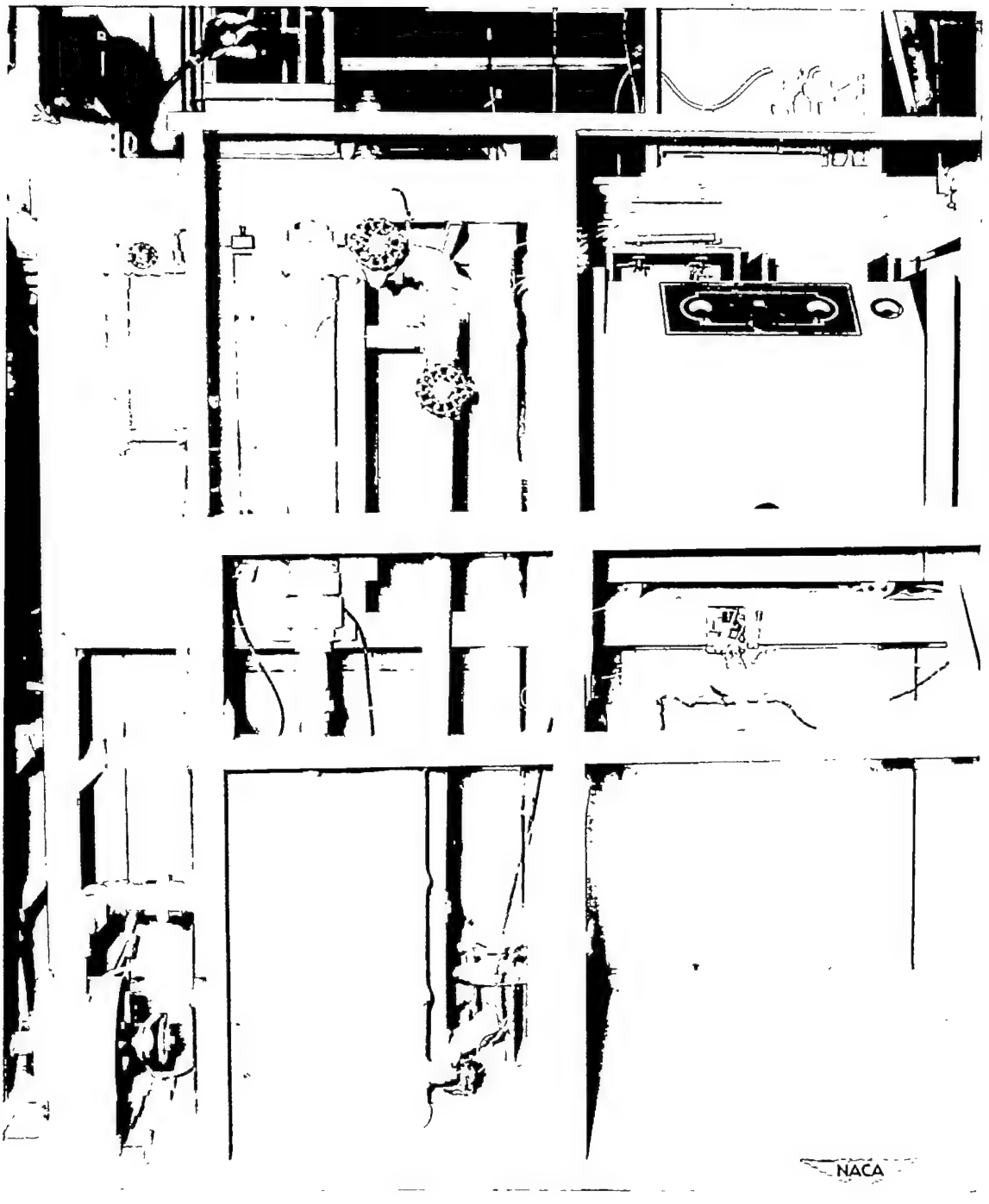

Figure 1.- Apparatus for heat-transfer measurements.

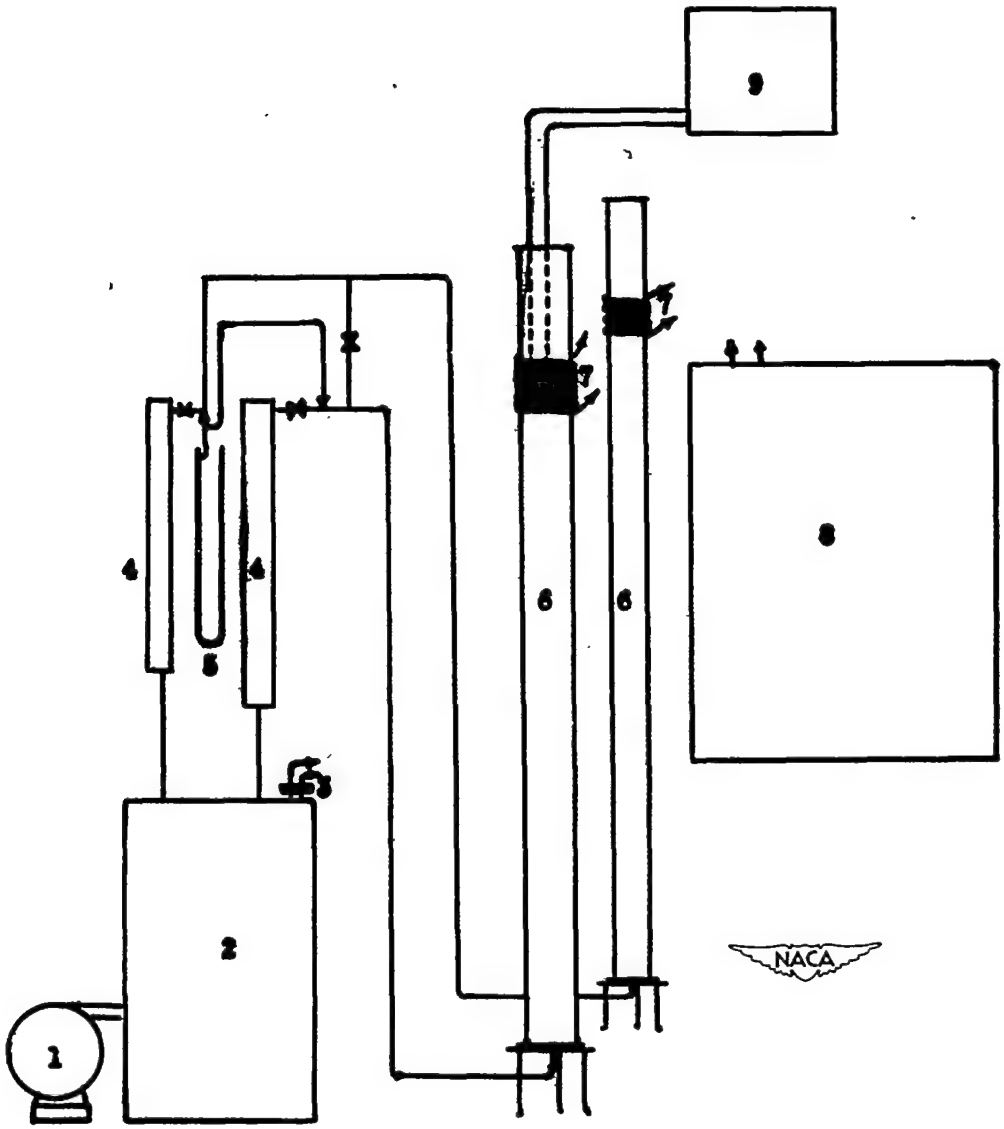

Figure 2.- Schematic diagram of apparatus for heat-transfer measurements. 1, blower; 2, surge tank; 3, air heater and temperature regulator; 4, rotameter; 5, manometer; 6, glass column; 7, heating coil; 8, Westinghouse R-F generator; and 9, potentiometer.

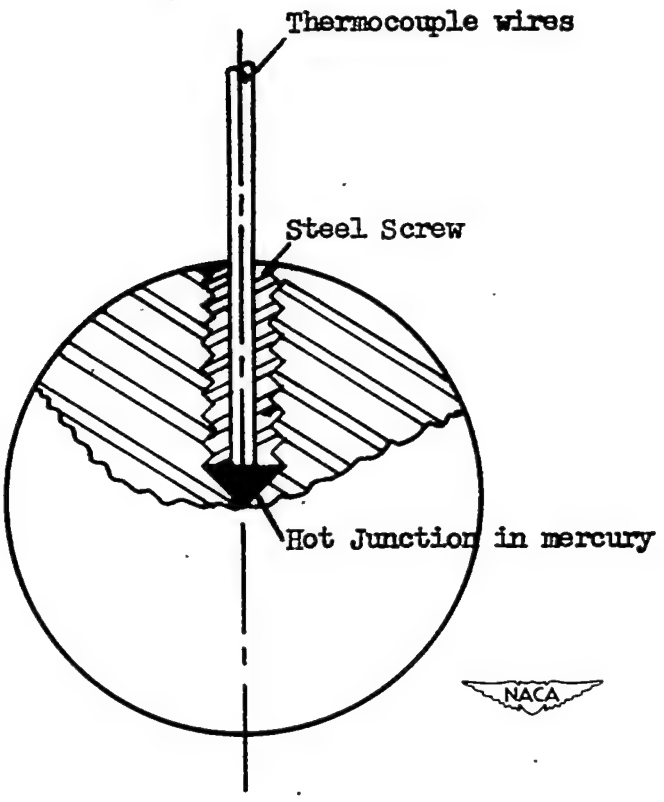

Figure 3.- Sectional view of spherical particle with hot junction of thermocouple attached. Four times full scale.

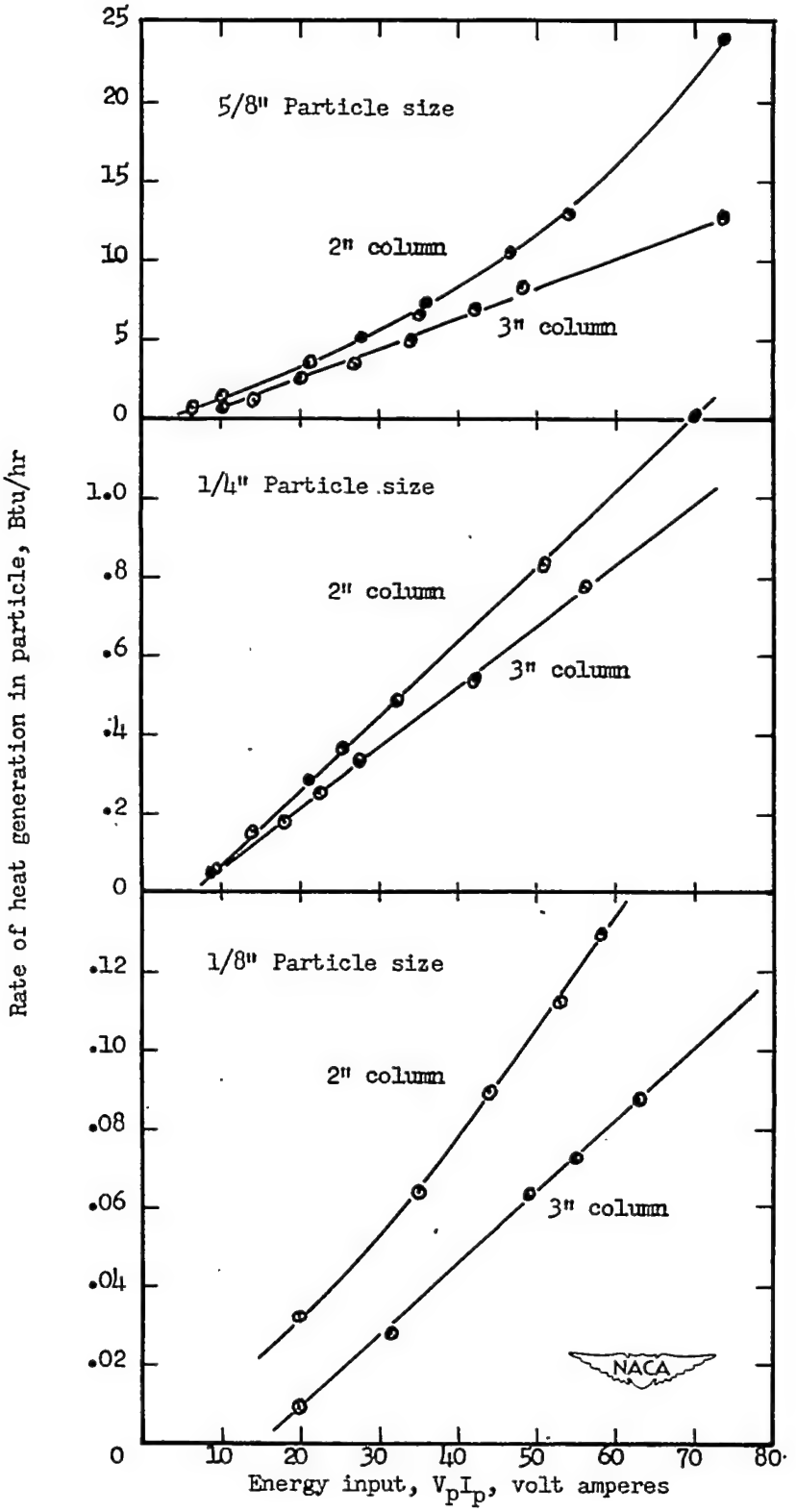

Figure 4.- Calibration curves for heating unit.

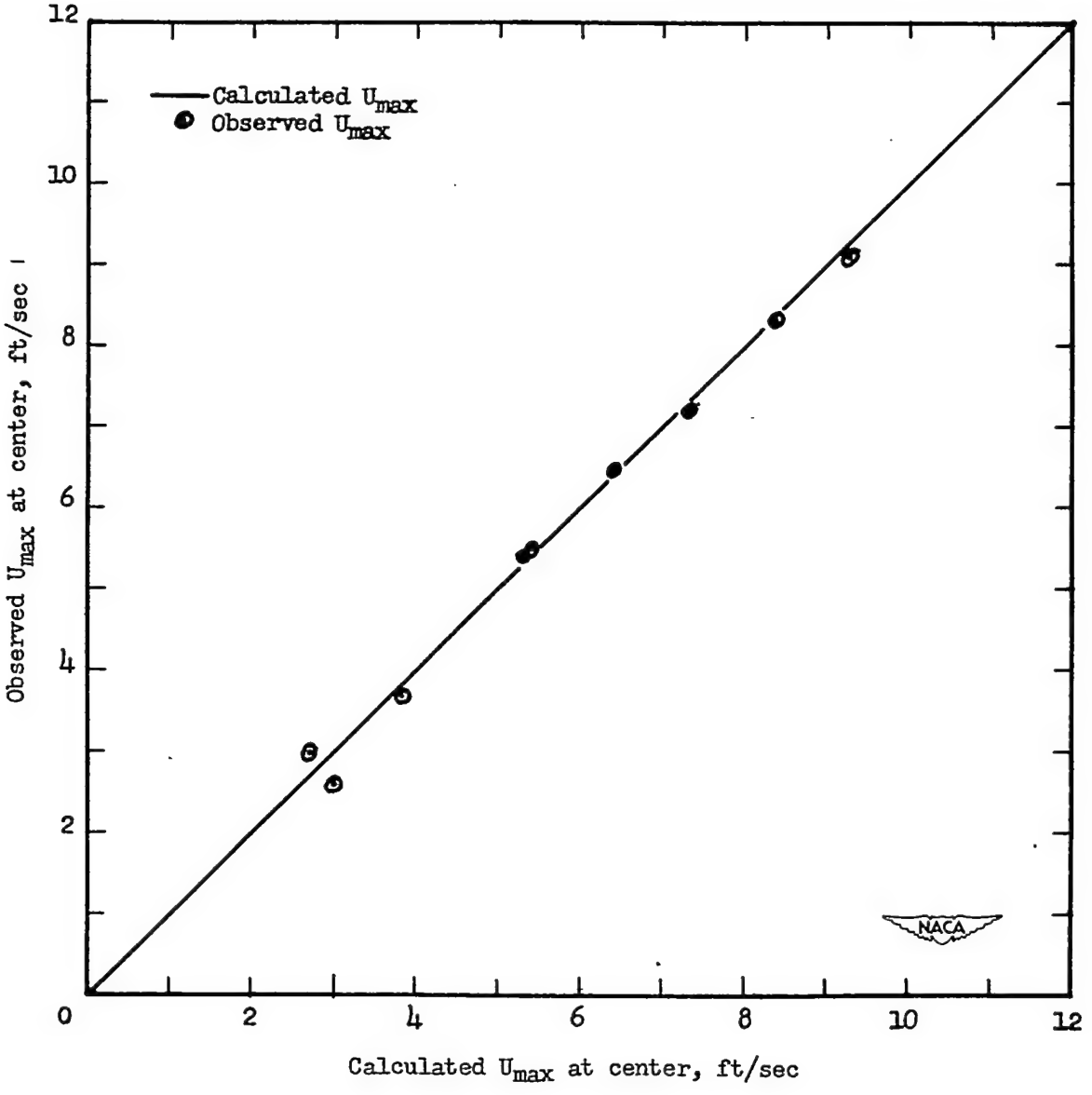

Figure 5.- Comparison of observed U_{max} and values of U_{max} calculated from flow-rate measurement at center of column.

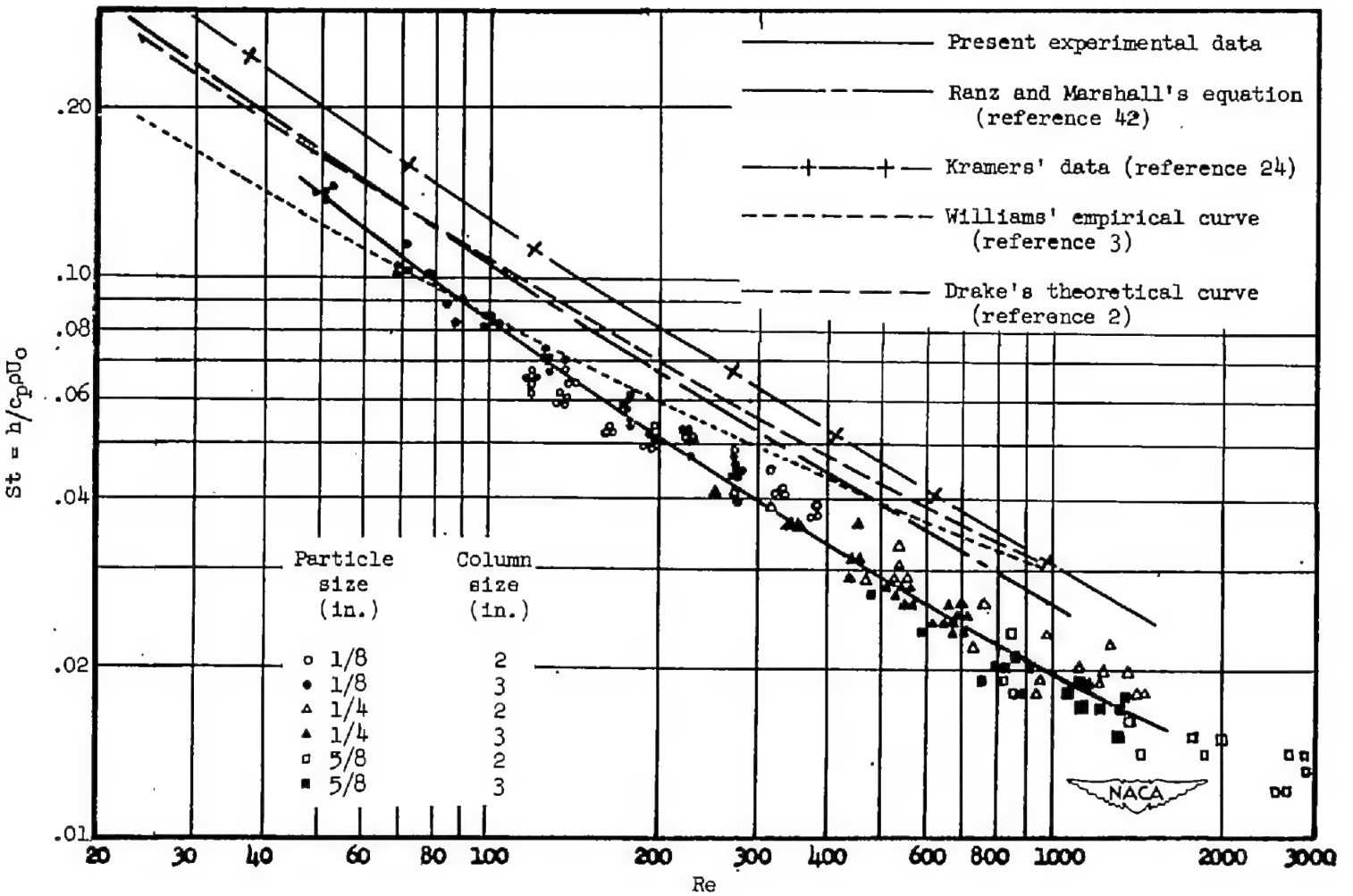

(a) Re against St.

Figure 6.- Comparison of experimental results with available heat-transfer data.

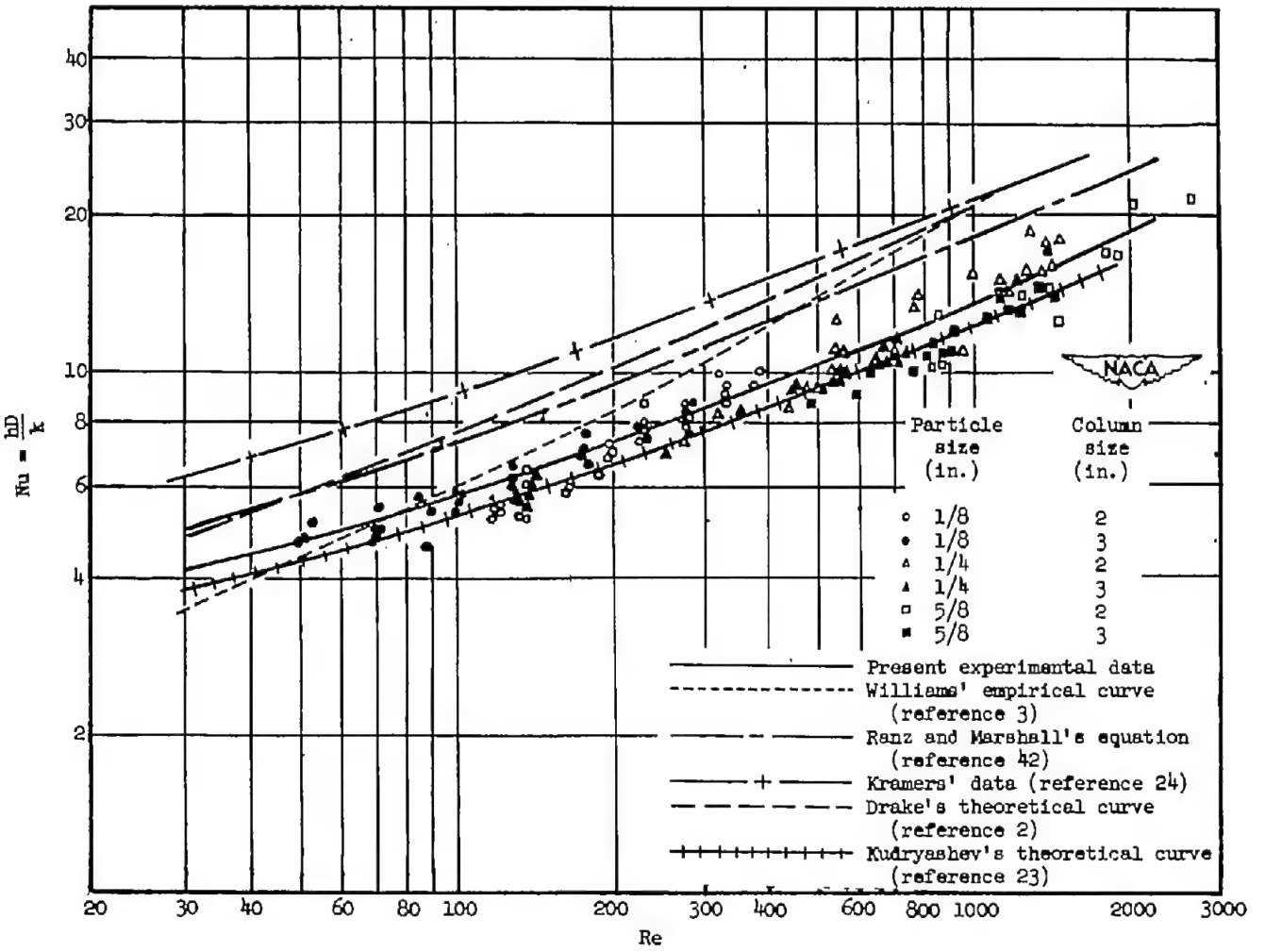

(b) Re against Nu.

Figure 6.- Concluded.

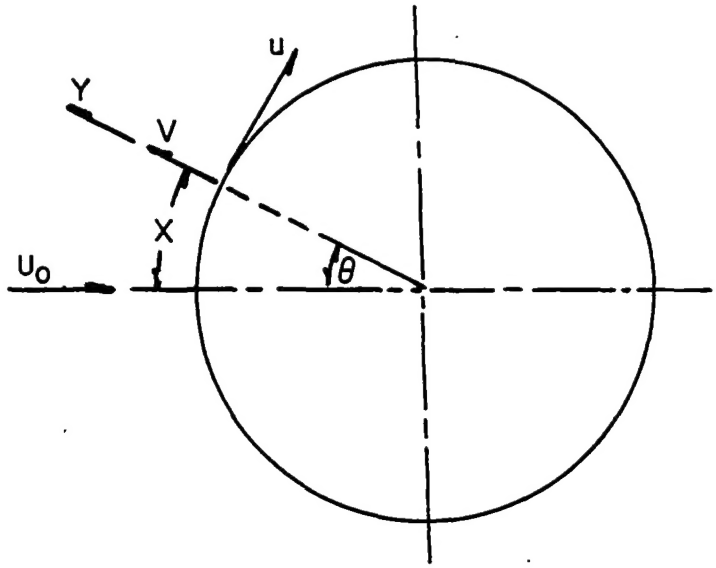

(a) Orthogonal coordinates.

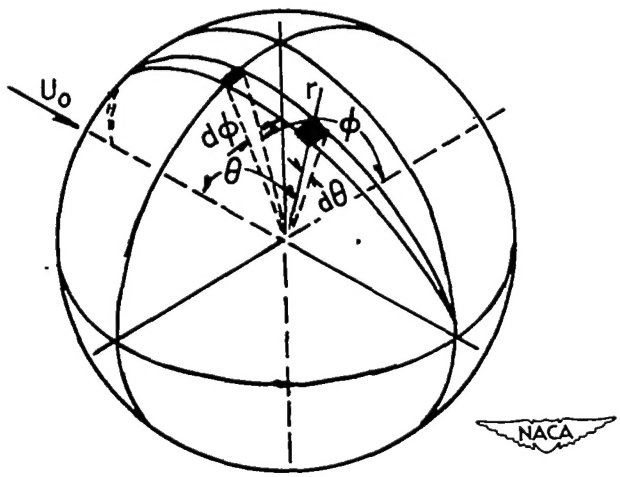

(b) Spheric coordinates.

Figure 7.- Orthogonal and spheric coordinates for spheres.

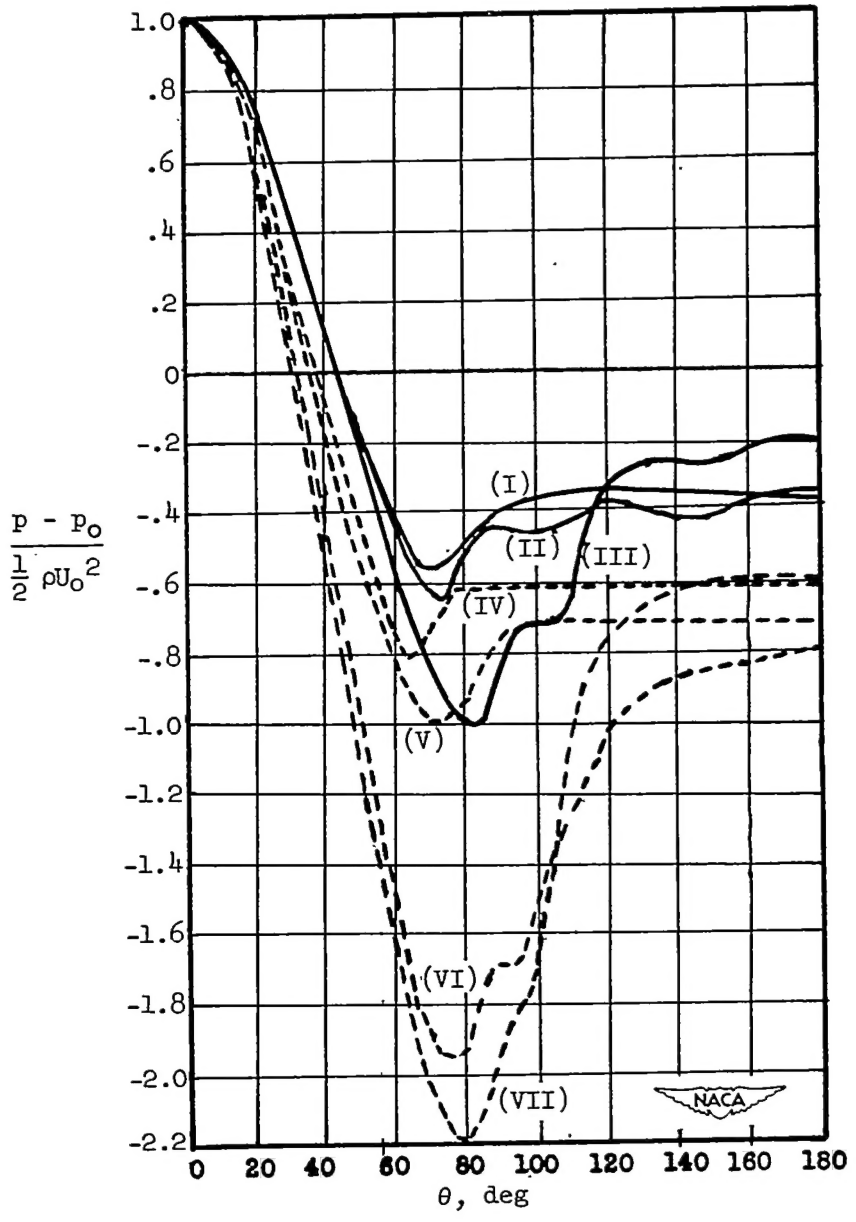

Sphere			Cylinder		
Curve	Source	R_e	Curve	Source	R_e
(I)	Flachsbart (reference 40)	16.5×10^4	(IV)	Giedt (reference 19)	7.08×10^4
(II)	Reference 21	15.7	(V)	Reference 21	.280
(III)	Reference 21	25.1	(VI)	Reference 21	21.2
			(VII)	Reference 21	16.6

Figure 8.- Pressure-distribution curves over a sphere and a cylinder.

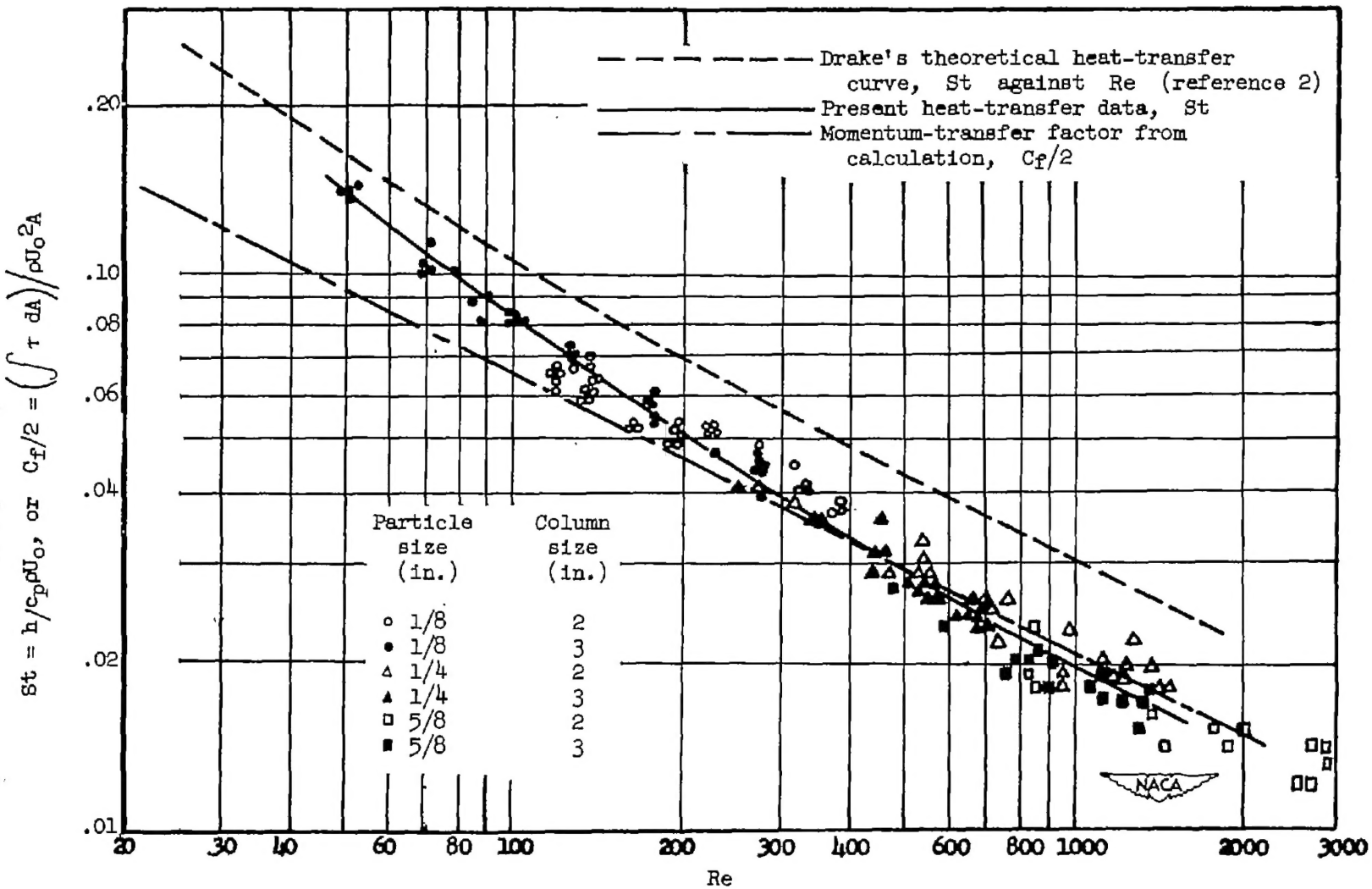

Figure 9.- Plot of heat-transfer factor St or momentum-transfer factor $C_f/2$ against Reynolds number Re.

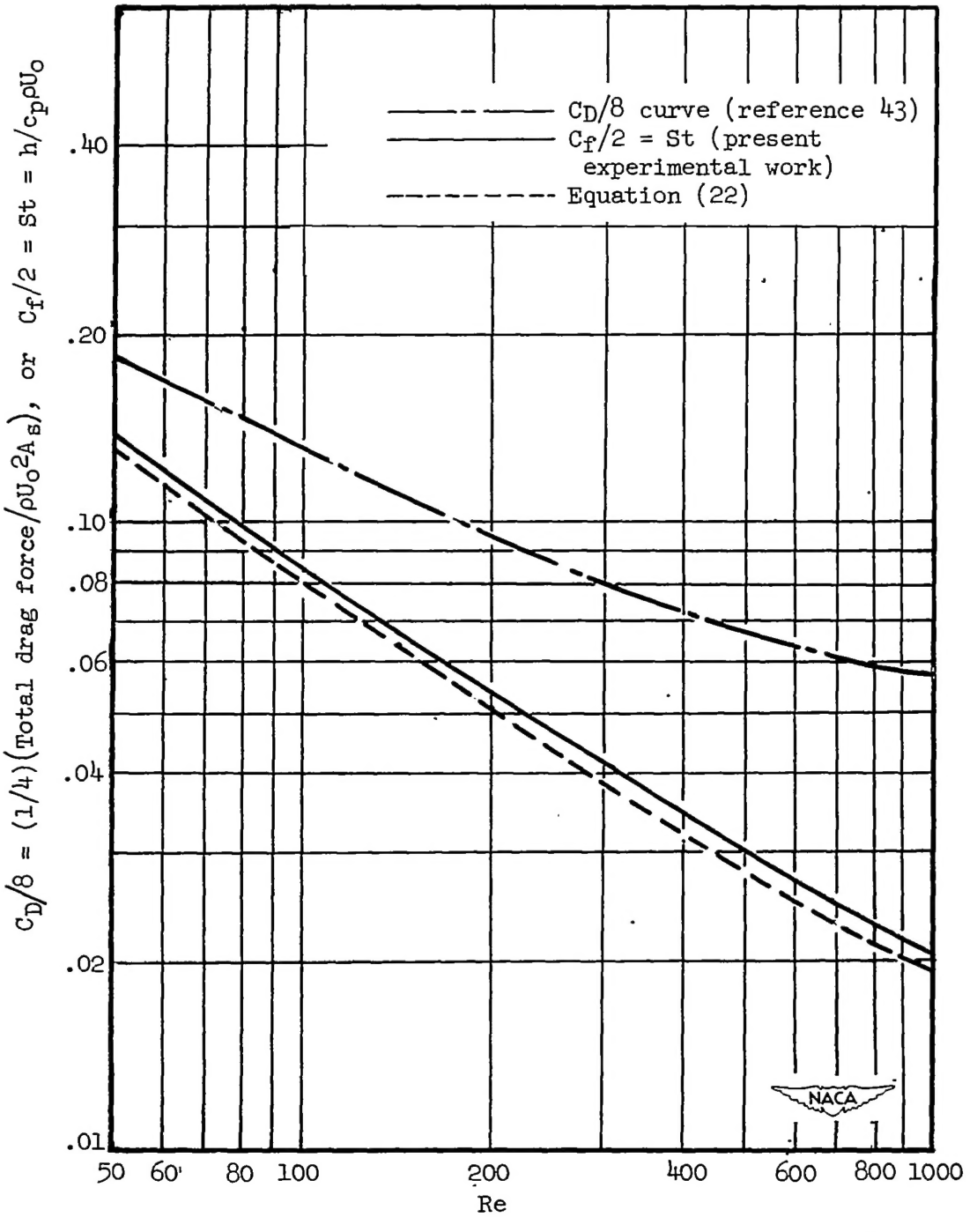

Figure 10.- Comparison of total-drag-coefficient function $C_D/8$ with momentum-transfer factor $C_f/2$ or heat-transfer factor St.

NACA-Langley - 9-2-54 - 120